

Review

Expression of active tectonics in erosional landscapes

Eric Kirby^{a,b,*}, Kelin X. Whipple^c

^a Department of Geosciences, Penn State University, University Park, PA 16803, USA

^b Department of Earth and Environmental Sciences, University of Potsdam, Potsdam 14476, Germany

^c School of Earth and Space Exploration, Arizona State University, Tempe, AZ 85287, USA

ARTICLE INFO

Article history:

Received 30 June 2011

Received in revised form

26 June 2012

Accepted 31 July 2012

Available online 7 August 2012

Keywords:

Tectonic geomorphology

Active tectonics

River profiles

Neotectonics

ABSTRACT

Understanding the manner and degree to which topography in active mountain ranges reflects deformation of the Earth's surface remains a first order goal of tectonic geomorphology. A substantial body of research in the past decade demonstrates that incising channel systems play a central role in setting relationships among topographic relief, differential rock uplift rate, and climatically modulated erosional efficiency. This review provides an introduction to the analysis and interpretation of channel profiles in erosional mountain ranges. We show that existing data support theoretical expectations of positive, monotonic relationships between channel steepness index, a measure of channel gradient normalized for downstream increases in drainage area, and erosion rate at equilibrium, and that the transient response to perturbations away from equilibrium engenders specific spatial patterns in channel profiles that can be used to infer aspects of the forcing. These aspects of channel behavior lay the foundation for a series of case studies that we use to illustrate how focused, quantitative analysis of channel morphology can provide insight into the spatial and temporal dynamics of active deformation. Although the complexities of river response to climate, lithology, and uplift patterns mean that multiple interpretations of topographic data alone will always be possible, we show that application of stream profile analysis can be a powerful reconnaissance tool with which to interrogate the rates and patterns of deformation in active mountain belts.

© 2012 Published by Elsevier Ltd.

1. Motivation

Geomorphology has long played a central role in the study of active fault systems. From early studies of the growth of fault-related folds (e.g., Rockwell et al., 1984), to the reconstruction of paleoseismic events from fault scarps (e.g., Wallace, 1977), to determinations of displacement rates along fault systems (e.g., Lensen, 1964), the landscape contains an important archive of the rates and spatial distribution of deformation. In the decades since these pioneering studies, advances in the dating of surficial deposits (Gosse and Phillips, 2001), in the characterization of fault slip (largely enabled by high-resolution remote sensing) (Gold et al., 2009; Klinger et al., 2011; Peltzer and Tappan, 1988; Tappan and Molnar, 1977), and in the high-precision determination of surface velocity fields (e.g., Dixon et al., 1995; Hager et al., 1991; Zhang et al., 2004) have fueled a resurgence in studies of active tectonics. The rates and patterns of fault slip provided by such studies constitute a framework upon which our current understanding of lithospheric deformation is built

(e.g., Davis et al., 2006; Meade and Hager, 2005), and, in some cases, geomorphic constraints highlight critical gaps in that understanding (e.g., Grant-Ludwig et al., 2010; Zielke et al., 2010).

A parallel revolution has been taking place in the study of topography in tectonically active erosional landscapes. Fueled by the recognition that the surface boundary conditions significantly influence the geodynamics of active orogens (e.g., Beaumont et al., 1992; Dahlen and Suppe, 1988; Koons, 1989, 1990; Whipple, 2009; Willett, 1999), study of the tectonic geomorphology of erosional landscapes has made remarkable progress in recent years. To a large degree, advances in the field have been enabled by rapid improvements in the digital representation of topography (e.g., Fielding et al., 1994) and in the measurement of erosion rates (e.g., Bierman and Steig, 1996; Granger and Riebe, 2007) such that we are now able to characterize the adjustment of the earth's surface topography to erosion rate with unprecedented precision. Collectively, this body of work largely confirms early notions (Davis, 1899; Penck, 1953) that landscape topography encodes information about the spatial and temporal patterns, and in some cases the rates, of differential uplift of rock (Wobus et al., 2006a and references therein).

This review focuses on this latter aspect of the field of tectonic geomorphology, the interpretation of landscape topography as a guide to active deformation. We are largely motivated by our

* Corresponding author. Department of Geosciences, Penn State University, University Park, PA 16803, USA.

E-mail address: ekirby@psu.edu (E. Kirby).

sense that the field is now on a relatively stable empirical and theoretical foundation and that focused analysis of topography can be a powerful tool with which to investigate questions of interest to the structural geology and tectonics community. The field is now poised to address questions ranging from the identification of active faults within the high-relief cores of active ranges (e.g., Kirby et al., 2003), to the growth and interaction of individual fault strands (Cowie et al., 2006), to the spatial and temporal patterns of rock uplift and deformation at orogenic scales (e.g., Schoenbohm et al., 2004; Wobus et al., 2003). However, no facile inversion of topography for uplift patterns and uplift history is yet possible given uncertainties in the physics of river incision and complexities in river response to climate, lithology, and uplift patterns in both space and time. This review provides a guide to the current state of the art in the analysis and interpretation of topography in tectonically active orogens.

2. Focus and scope

The traditional approach to tectonic geomorphology, the use of landforms as markers of deformation, remains the gold standard for the characterization of active deformation along faults (e.g., Behr et al., 2010; Zielke et al., 2010) and across growing folds (e.g., Lavé and Avouac, 2000). However, the requirements that such markers retain remnants of their initial geometry (Burbank and Anderson, 2001), means that features appropriate for reconstruction of deformation are rather rare in rapidly eroding mountain ranges. Moreover, because degradation of initial depositional surfaces strongly influences approaches to exposure dating (e.g., Hidy et al., 2010), the utility of most landforms as a measure of displacement rates is often limited to the past 50–100 kyr. In addition, it is increasingly recognized that the formation of such markers is strongly modulated by local and global changes in climate (e.g., Bacon et al., 2009; Pan et al., 2003; Van der Woerd et al., 2002) and the consequent regional synchrony of fluvial terraces, alluvial fan surfaces, and/or glacial moraines leads to the potential for aliasing of deformation rates at various timescales (c.f., Grant-Ludwig et al., 2010).

In contrast, the erosional response to deformation of the earth's surface provides an integrated record of relative changes in rock uplift (measured relative to a fixed, external baselevel) (England and Molnar, 1990). Topographic relief has long been recognized to hold clues to the pattern of differential motion of rock (e.g., Wager, 1933, 1937), and correlations between relief and erosion rate (Ahnert, 1970) suggest that landscape relief may adjust such that erosion rates attain an equilibrium with the uplift of rock (e.g., Adams, 1985). However, it is now widely appreciated that landscape relief in most actively eroding orogens (below the glacial limit) is set by the longitudinal profiles of the channel network (Whipple et al., 1999). Because hillslopes rapidly attain threshold gradients in actively eroding mountain ranges (Burbank et al., 1996; Clarke and Burbank, 2010; Densmore et al., 1997; Schmidt and Montgomery, 1995; Strahler, 1950), the degree to which channel profiles adjust their profile shape in response to spatial and temporal changes in rock uplift rate (Whipple and Tucker, 2002, 1999) exerts a first-order control on orogen-scale relief (e.g., DiBiase et al., 2010).

The channel network in active orogens also dictates the pace at which landscapes respond to changes in forcing driven by changes in baselevel (tectonic, eustatic, or drainage reorganization) and/or in climate state. The rate at which these signals move through the channel network is a function of the processes that control incision of rivers into bedrock (Rosenbloom and Anderson, 1994; Whipple, 2004), as well as the magnitude and direction of the perturbation (Niemann et al., 2001; Whipple, 2001). Because rivers set the lower

boundary condition for hillslopes throughout a watershed, incision along the channel network dictates the local rate of baselevel fall experienced by each hillslope. This rate directly influences the amount and probably caliber of sediment delivered to the channel, and because strong feedbacks likely exist between river incision, channel slope, bed state, and grain size (Johnson and Whipple, 2007; Sklar and Dietrich, 1998, 2004; Turowski et al., 2007; Whittaker et al., 2010), the coupling between channel incision and sediment delivery may modulate the response time of channel systems to perturbations (Whipple and Tucker, 2002).

This review has three primary goals: 1) to provide an introduction to the analysis and interpretation of channel topography in erosional mountain ranges, 2) to show, by example, how such studies can provide insight into the spatial and temporal dynamics of active deformation, and 3) to highlight current gaps in our understanding that hinder interpretation. Because of the central role of bedrock channels in the evolution of topography, this review is largely restricted to fluvial systems although we note there are important differences among glaciated landscapes (Brocklehurst and Whipple, 2007; Foster et al., 2010; Oskin and Burbank, 2005). We build on previous reviews of the processes of fluvial incision (Whipple, 2004), the interpretation of scaling relationships in channel systems (Wobus et al., 2006a), and the role of bedrock channels in landscape relief (Whipple et al., 2011). Similarly, we do not address the dynamic feedbacks between climate, erosion and tectonics at an orogen scale (Whipple, 2009 and references therein). Although quantitative knowledge of the full range of processes that control weathering, erosion, and transport of sediment in fluvial systems is far from complete, recent progress in understanding key aspects of these systems such as the combined effects of transport or incision thresholds and runoff variability (c.f., Lague et al., 2005; Tucker, 2004), provides some grounds for optimism that erosional topography retains an interpretable signature of tectonic forcing. As we show below, the successes of numerous studies relating channel profile morphology in both steady-state mountain belts (those where erosion is in approximate balance with the uplift of rock – Willett and Brandon, 2002) and in ones that are experiencing an ongoing adjustment to a change in external forcing is encouraging.

3. Fluvial systems as recorders of active tectonics

3.1. Background – the graded profile

As noted above, the shape of river profiles largely dictates topographic relief in erosional landscapes. Although the concept of a "graded" river dates to the early days of geomorphology (Davis, 1902; Gilbert, 1877), it was best articulated by Mackin (1948) who described a graded stream as one in which the "slope is delicately adjusted to provide, with available discharge and the prevailing channel characteristics, just the velocity required for transportation of all the load supplied from above". This perspective, that the landscape expresses a dynamic equilibrium between the rates of material supply (typically, the uplift of rock) and the rates of removal, still underpins modern geomorphic thought (e.g., Dietrich et al., 2003; Snow and Slingerland, 1987). As first noted by Hack (1957), most graded river profiles are well-described by a power-law relationship between local channel slope (S) and the contributing drainage area upstream (A),

$$S = k_s A^{-\theta} \quad (1)$$

where k_s is referred to as the channel steepness index and θ as the concavity index (Flint, 1974). Because the shape of the catchment upstream strongly influences the rate at which discharge increases

downstream, it consequently influences the rate at which slopes change along a river (Fig. 1), which of course is the concavity of the profile itself (Hack, 1957). Thus, most workers use the term “concavity index” to refer to the exponent in Equation (1) (c.f., Wobus et al., 2006a) to distinguish it from the actual concavity of the profile (c.f., Demoulin, 1998).

The scaling relationship expressed in Equation (1) strictly only holds downstream of a critical threshold drainage area (A_{crit}), typically observed to fall in the range of 0.1–5 km² (Montgomery and Foufoula-Georgiou, 1993; Wobus et al., 2006a). Over this range of drainage area, a transition occurs from hillslopes and colluvial channels thought to be dominated by debris-flows (Stock and Dietrich, 2003) to fluvial channels. This transition may be either abrupt or gradual. Regardless, this transition is commonly recognized as a change in scaling from a region where slopes are largely invariant with increasing drainage area, to one where slopes decrease systematically downstream (Stock and Dietrich, 2003; Wobus et al., 2006a). Downstream of the transition, where Equation (1) holds, however, it is important to recognize that abrupt spatial or temporal changes in substrate lithology, rock uplift rate, and/or climate may lead to development of a segmented profile. Typically, each segment exhibits scaling relationships similar to Equation (1), but with varying values of steepness index (k_s), concavity index (θ), or both (Wobus et al., 2006a). Often the characteristics and spatial distribution of such segments across the landscape and in channels of different size and orientation hold the key to deciphering the spatial and temporal history of rock uplift

and for disentangling the complicating influence of substrate properties, sediment load characteristics, and precipitation patterns.

Although the significance of variability in the concavity index in natural streams has been the subject of significant debate (Moglen and Bras, 1995; Sklar and Dietrich, 1998; Tucker and Whipple, 2002), three key points emerge. First, analyses of stream profiles in simple settings, with uniform substrate, uplift rate (and pattern), and climate reveal that concavity indices fall within a relatively narrow range (~0.4–0.6 – Duvall et al., 2004; Kirby and Whipple, 2001; Snyder et al., 2000; Whipple, 2004; Wobus et al., 2006a). Second, systematic downstream changes in 1) rock uplift rate (Kirby and Whipple, 2001), 2) lithology (Duvall et al., 2004; Moglen and Bras, 1995), 3) the extent of alluvial cover of the bed (Sklar and Dietrich, 2004, 2006), and/or 4) runoff (Craddock et al., 2007; Roe et al., 2002; Schlunegger et al., 2011; Zaprowski et al., 2005) can influence the concavity index. Third, simple models of river incision predict that where uplift and lithology are uniform, the concavity index is largely set by the relative rates of downstream increase in discharge versus channel width (Whipple, 2004; Whipple and Tucker, 1999) and is not strongly dependent on the presence of incision thresholds (Lague et al., 2005; Tucker, 2004). Thus, although the complexities above are often expressed in natural channels, there is good reason to expect that the shape of a graded profile has a relatively restricted range of concavity (see further discussion in Whipple et al., 2011).

3.2. Indices of channel steepness

The observation that the concavity index (θ) is relatively insensitive to differences in rock uplift rate, climate or substrate lithology at steady-state (provided such differences are uniform along the length of the channel) but that the steepness index (k_s) varies with these factors (e.g., Kirby and Whipple, 2001; Wobus et al., 2006a) makes this latter index a useful metric for tectonic geomorphic studies. In this section, we first discuss historic approaches to using channel gradients as a gauge of tectonic activity (e.g., Hack, 1973), and then demonstrate how analysis of channel profiles using Equation (1) can yield insight into the relative rates of rock uplift in erosional landscapes.

3.2.1. Hack's stream gradient (SL) index

In his seminal work on the longitudinal profiles of rivers in the Appalachians, John Hack (1957) argued that most rivers followed a semi-logarithmic profile, of the form:

$$z(x) = k_h \ln(x) \quad (2)$$

where z is elevation of the river profile, x is distance downstream, measured along the thalweg of the stream, and k_h is a constant referred to as the gradient index. Differentiating with respect to distance yields an expression for channel slope as a function of distance:

$$S(x) = k_h 1/x \quad (3)$$

Note the similarity between Equations (1) and (3). For typical basin shapes (shape sets the relation between A and x) and typical concavity indices (0.4 ≤ θ ≤ 0.6), Equation (1) approximately reduces to Equation (3); Equation (1) is simply a more general statement of Equation (3). Hack made this approximation because continuous measurements of upstream drainage area along a channel were impractical prior to the development of digital elevation models (DEMs). One can determine the value of the Hack gradient index a given distance along the channel, L , via:

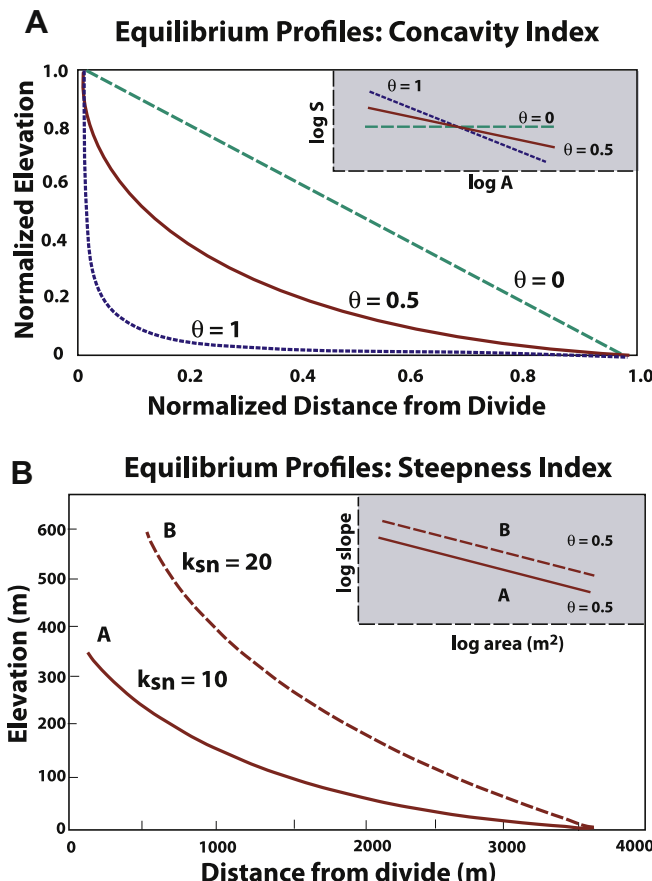


Fig. 1. Schematic representation of channel profile form (modified from Duvall et al., 2004; Whipple and Tucker, 1999). (A) Example showing the influence of concavity index (θ) on both profile shape and slope-area scaling (inset). (B) Comparison of two profiles with varying steepness indices (k_{sn}), but identical concavity indices.

$$SL = k_h \quad (4)$$

a quantity readily measured directly from topographic maps. This approach has been a useful guide to evaluating departures of channel profiles from an idealized form (Hack, 1973), and was the origin of initial successes in evaluating tectonic activity in erosional settings. In a groundbreaking analysis, Seeber and Gornitz (1983) argued that a spatial coincidence among steep channels with high SL indices, microseismicity, and high topography along the arc of the Himalaya reflected ongoing rock uplift above an active fault beneath the range, a result largely confirmed by geodetic leveling (Jackson and Bilham, 1994) and GPS in recent decades (Bettinelli et al., 2006; Larson et al., 1999). Although the details of the distribution of deformation, and whether it reflects deformation and rock uplift above a ramp in the main decollement between India and Asia (Jackson and Bilham, 1994), passive uplift of rock above a growing duplex (Avouac, 2003; Herman et al., 2010), or active surface-rupturing faults (Hodges et al., 2004; Wobus et al., 2005, 2003), remains a point of debate, there is little doubt that the analysis of Seeber and Gornitz (1983) was prescient in its use of geomorphology to map patterns of active deformation. We will return to this topic as a case study in the application of geomorphic approaches to tectonic problems.

The SL index also found success in studies of coastal stream response to variations in rock uplift in California (Merritts and Vincent, 1989). Here, channels experiencing uplift rates ranging from 0.3 to 4 mm/yr exhibited strong differences in SL index, suggesting that these channels were adjusted to the prevailing tectonic forcing (Merritts and Vincent, 1989). However, this same study highlighted the shortfalls of simply comparing channel gradients, without normalizing for differences in drainage area (and thus, discharge). In a comparison of first-, second- and third-order streams, these authors concluded that the degree of gradient adjustment depended on the size of the catchment (Merritts and Vincent, 1989). This conclusion and its corollary, that channel concavity should increase with increasing rates of rock uplift, are now known to be incorrect (Snyder et al., 2000). As discussed below, this example illustrates the need to normalize channel gradients for downstream changes in discharge in order to effect comparisons among channels experiencing different climatic and tectonic forcing.

Despite these early successes, the Hack gradient index is limited by its dependence on the formal choice of equilibrium profile shape. It is self-evident from Equations (2)–(4) that any deviation in the shape of the river profile away from a semi-log relationship will lead to SL indices that vary systematically along the stream. Because such variation may arise as the consequence of small differences in basin shape (Fig. 2), interpretations based on this index alone should be viewed with caution. A similar approach was proposed by Bishop et al. (2005) that exploits the fact that channel slope tends to vary systematically as a power function of downstream distance (Hack, 1957), independent of whether or not the profile follows a semi-log relationship. Although this method provides a more general framework for the analysis of longitudinal profiles, the dependence on basin shape remains (Goldrick and Bishop, 2007), such that small differences in the way discharge accumulates downstream will lead to systematic variations in this gradient index. As we show below, one way to surmount this dependence is provided by indices that rely on channel slope and drainage area (e.g., Wobus et al., 2006a).

3.2.2. Channel steepness indices derived from analysis of slope-area data

In practice, determination of the concavity index (θ) and steepness index (k_s) can be accomplished by linear regression of gradient against drainage area on a log–log plot (Fig. 1) (Wobus

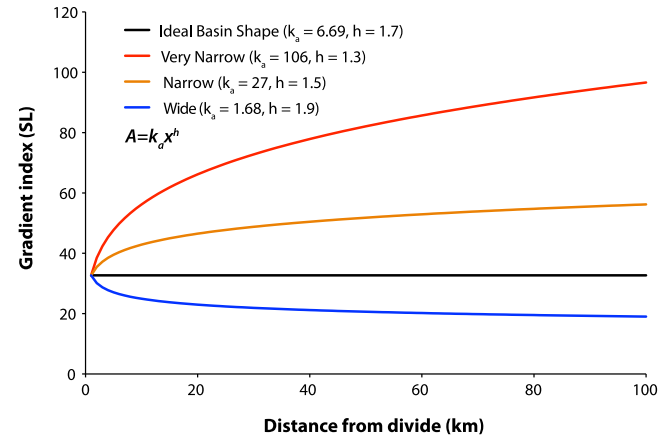


Fig. 2. Influence of basin shape on the Hack gradient index (SL). This dependence arises because of the way in which discharge accumulation downstream sets equilibrium gradients.

et al., 2006a). However, because small variations and/or uncertainties in the concavity index (regression slope) lead to wide variations in the steepness index (regression intercept), one needs to develop a normalized index that accounts for this autocorrelation. Two methods have been proposed. The first of these was suggested by Sklar and Dietrich (1998), and simply involves calculating a reference slope (S_r) by evaluating Equation (1) at a fixed, reference drainage area (A_r):

$$S_r = k_s A_r^{-\theta} \quad (5)$$

This is an effective and simple way to compare gradients among streams of similar size, and is most reliable when A_r is located at or near the centroid of the data used in regression (Sklar and Dietrich, 1998). However, the requirement of choosing a single drainage area makes comparison of drainages of widely varying size difficult, which is unfortunate since contrasting the response of small and large rivers is often essential for isolating tectonic influences on landscape form (e.g., Kirby et al., 2003).

The second method exploits the expectation that concavity indices of steady-state channels should fall into a relatively restricted range ($0.4 \leq \theta \leq 0.6$). By evaluating slope-area regressions using a reference concavity index (θ_{ref}), one can determine a normalized steepness index (k_{sn}) that allows effective comparison of profiles of streams with greatly varying drainage area (Wobus et al., 2006a):

$$S = k_{sn} A^{-\theta_{ref}} \quad (6)$$

This method is thus a means of determining channel slopes that have been corrected for the expected dependence of profile gradient on drainage area (Wobus et al., 2006a).

In a manner similar to the reference slope method (Sklar and Dietrich, 1998), the normalized steepness index (k_{sn}) effectively determines a value representative of the centroid of the data bound by the upstream and downstream limits of the regression. In practice, this means that the value that one determines for a given segment of a channel depends, in part, on how one chooses to define regression limits. Although the simplest approach, and common practice (e.g., Snyder et al., 2000) is to use a single regression from headwaters to the mountain front, as noted above, many channels are segmented by variations in lithology and/or uplift rate (in space or time). Recognizing the segmented nature of river profiles and choosing these limits is an integral part of any tectonic interpretation and is discussed below.

The analysis of channel gradients described above relies heavily on digital elevation models (DEMs). These data are inherently noisy, however, and many of the data handling methods were developed in response to the need to reduce scatter in raw pixel-to-pixel slope estimates from DEMs (Wobus et al., 2006a). The relatively large scatter in pixel–pixel slope estimates stems from relatively minor noise in the long profiles extracted from DEMs; taking the spatial derivative of course exaggerates this noise. Most current analysis protocols attempt to reduce this noise through a combination of: sub-sampling the long profile, fitting piece-wise linear regressions to the long profile to estimate local slope, applying a moving-average filter to long profile data, and taking log A-bin averages of log S (Shahzad and Gloaguen, 2011; Wobus et al., 2006a). Interested readers can obtain open-source codes that are tailored to these analyses in several places; the authors' codes are available from <http://www.geomorphotools.org> and similar ones developed at the University of Freiberg at <http://www.rsg.tu-freiberg.de/twiki/bin/view/Main/TecDEM>.

A third approach to measuring channel steepness was proposed independently by Royden et al. (2000) and Sorby and England (2004). Instead of differentiating the long profile to derive an estimate of S , one can integrate both sides of Equation (1) to write:

$$z(x) = k_s \int_0^x A(x')^{-\theta} dx' \equiv k_s \chi(x) \quad (7)$$

The transformed variable $\chi(x)$ can be determined directly from drainage area data by numerical integration (see discussion in appendix of Harkins et al., 2007). As such, we refer to this as the integral method of determining channel steepness.

In the integral method, segments of the channel profile which are well described by a concavity index equal to θ will be linear on plots of z vs. χ . The slope of this line gives the value of the steepness index, k_s . Segments of the channel profile, however, that are not well described by a power-law relation between channel gradient and upstream drainage area, or segments with a concavity index different from the reference value of θ , will be curved. Standard linear regression can be used to both evaluate linearity of channel segments (by searching for correlated residuals, Bevington and Robinson, 1992), to estimate k_s , and to accurately determine uncertainties on this value. However, as the best-fit value of θ is not known *a priori*, in principle one must either use standard $\log S - \log A$ relations to find θ , or compute $\chi(x)$ for a range of θ values and test for linearity over the channel segment of interest. In practice we have found that values of θ_{ref} between 0.4 and 0.5 work well for most mountain rivers. $\theta_{ref} = 0.45$ is used in most of the literature to date.

3.3. Channel adjustment to rock uplift: the theoretical perspective

Since the introduction of the shear-stress river incision model (Howard and Kerby, 1983), a variety of fluvial incision models have been proposed. Most of these are phenomenologic (Howard, 1994; Snow and Slingerland, 1987) in that they attempt to describe the physics of incision processes (Hancock et al., 1998; Whipple et al., 2000) and their interactions (Johnson and Whipple, 2007) in terms of the overall dependence of incision rate on local fluid shear stress on the channel bed combined with measures of rock strength and flood statistics. In this section, we provide only the briefest of reviews of these models and emphasize their predictions for how river profiles adjust to tectonic forcing. For a more comprehensive discussion of the problem of fluvial incision into bedrock, and progress in the modeling of this complex morphodynamic system, the reader is referred to recent reviews (Whipple, 2004; Whipple et al., 2011).

By far, the most commonly used river incision models are from the “stream-power” family of models (Howard, 1994; Whipple and Tucker, 2002, 1999). Although this class of models is not process specific, it has proven useful as a framework for guiding investigations of channel form in active mountain belts (e.g., Snyder et al., 2000). Moreover, various forms of process-specific models (e.g., Lague, 2010; Sklar and Dietrich, 1998, 2004, 2006) can be cast as variations of the stream-power model (Gasparini et al., 2007; Whipple, 2004). In this family of models, the erosion rate (E) along the bed of a channel is posited to vary as a power function of mean bed shear stress (τ_b) (Howard and Kerby, 1983; Whipple and Tucker, 1999). When this stress exceeds a critical threshold for detachment of rock or initiation of bedload motion (τ_c), whichever is greater, an expression for bed erosion rate can be written as:

$$E = k_e f(q_s) [\tau_b^a - \tau_c^a] \quad (8)$$

where k_e depends on substrate properties, $f(q_s)$ is a function that describes the modulating effects of sediment load (Lague, 2010; Sklar and Dietrich, 1998, 2004; Whipple and Tucker, 2002), and the exponent a depends on the mechanics of erosion (Howard and Kerby, 1983; Whipple et al., 2000). Under conditions of steady, uniform flow, the shear stress exerted by the fluid on the bed can be approximated in terms of water discharge (Q), channel bankfull width (W) and bed slope (S) (Howard, 1994):

$$\tau_b = k_t (Q/W)^\alpha S^\beta \quad (9)$$

where k_t , α , and β are set by a flow resistance equation (typically, Manning's equation. See Whipple and Tucker, 1999). Combining Equation (9) with empirical relations among discharge, drainage basin area (A), and bankfull width leads to a generalized form of the stream-power family of incision models (Whipple, 2004):

$$E = KA^m S^n \quad (10a)$$

$$K = K_r K_c K_{tc} f(q_s) \quad (10b)$$

where K_r is set by k_e , k_t , and channel width, K_c is dictated by climatic regime, K_{tc} is a threshold term, and the exponents m and n are set by the exponents a (Equation (8)), α and β (Equation (9)), and the empirical relations among Q , A , and W (Whipple and Tucker, 1999). Importantly, the m/n ratio is predicted to depend only on the rate of increase of Q and W with drainage area, with a typical value of $\sim 1/2$.

At steady state, by definition the channel erosion rate is equal to the uplift rate of rock ($E = U$), and the steady-state channel gradient (S_e) can be found by solving Equation (10) for slope under this condition:

$$S_e = (U/K)^{1/n} A^{-m/n} \quad (11)$$

Equation (11) has the same form as Equation (1) and predicts $\theta \sim 1/2$, consistent with observations for well-graded channels with uniform K and U ($0.4 \leq \theta \leq 0.6$, Tucker and Whipple, 2002). Thus, the relatively restricted range of natural concavities observed in equilibrium settings (Duvall et al., 2004; Kirby and Whipple, 2001; Snyder et al., 2000; Wobus et al., 2006a) is probably due largely to the manner in which downstream increases in discharge and width modulate equilibrium gradients. Although process-based models that explicitly incorporate the dual role of coarse sediment as both tools (which facilitate impact-based wear of channel bed and walls) and cover (which shields the bed from wear) (e.g., Sklar and Dietrich, 1998) predict a slight dependence of steady-state channel concavity on erosion rate/rock uplift rate (Sklar and Dietrich, 2004, 2006; Turowski et al., 2007), at present no field-

based studies have been able to discern this effect through the noise of natural systems.

Despite differences in detail, all models predict monotonic increases in steady-state channel gradient with increasing rock uplift rate (Whipple, 2004). This adjustment directly depends on the exponents m and n , which are not free parameters, but rather reflect the mechanics of the dominant incision process, or combination of processes (Whipple, 2004). Although incision models which neglect a threshold for incision predict that steady-state channel gradients (and, channel steepness, k_{sn} in Equation (6)) should depend directly on the degree of non-linearity embedded in the incision process (Whipple et al., 2000) and parameterized in the exponent n (Whipple and Tucker, 1999), recent studies emphasize a critical role for an incision threshold in the relationships among channel steepness, climate, and tectonics (Lague et al., 2005; Snyder et al., 2003b; Tucker, 2004). These analyses highlight the significance of the probability distribution of runoff events; the combination of a threshold for incision and a distribution of discharge leads directly to a non-linear relationship between steady-state channel steepness and erosion rate. This relationship emerges because a greater portion of the flood distribution will generate shear stresses that exceed the threshold in steep channels, resulting in more efficient erosion. The detailed nature of this non-linearity, however, depends on the magnitude of the threshold itself and the rock uplift rate, as well as on the climate state and the nature of the runoff distribution (DiBiase and Whipple, 2011; Lague et al., 2005; Snyder et al., 2003b; Tucker, 2004).

Thus, although the form and parameterization of river incision models need to be more fully tested against field data, two central conclusions regarding the adjustment of channels to rock uplift rate can be drawn from the existing literature. First, channels developed within a given climate regime and upon substrate of similar strength are expected to exhibit a non-linear scaling between rock uplift rate and channel steepness (e.g., Snyder et al., 2003b):

$$k_{sn} \propto U^p \quad (12)$$

Second, the exact nature of this scaling (i.e., the exponent p) is expected to vary, perhaps widely, among field sites as differences in dominant erosion processes and differences in rock strength and/or erosion thresholds combined with differences in the frequency-magnitude distribution of runoff influence the efficiency of erosion (Lague et al., 2005). Model predictions can be tested against observations and used to refine understanding of river incision mechanics and the roles of climate and lithology in modulating the relationship between rock uplift and channel steepness. Moreover, Equation (12) and its dependence on climate and lithology are not only useful for testing models against data, but also encapsulate the key to quantitative understanding of the potential feedbacks between climate and tectonics in orogenesis (e.g., Whipple, 2009).

3.4. Channel adjustment to rock uplift: the empirical perspective

Despite our incomplete understanding of channel incision processes, there is strong empirical support for positive, monotonic functional relationships between channel steepness and erosion rate (Wobus et al., 2006a). Early studies relied on analysis of channel profiles in relatively simple field sites – those where rock uplift rates, and their spatial variability, were known independently. In coastal California, Snyder et al. (2000; 2003a, b) and Duvall et al. (2004) both studied small, coastal channels experiencing differences in rock uplift rate but developed in uniform bedrock and under uniform climate conditions. Notably, in both sites, channel concavity did not appear to depend on the rate of

rock uplift, provided that bedrock was uniform (Duvall et al., 2004), but channel steepness (k_{sn}) exhibited a non-linear relationship with rock uplift/erosion rate. These were interpreted to reflect the role of an incision threshold (Snyder et al., 2003b) and differences in channel width (Duvall et al., 2004) although Whipple (2004) offered an alternative explanation.

In contrast, studies of channel profiles developed across an actively growing fold in the Siwalik Hills of central Nepal suggest a linear relationship between channel steepness and erosion rate (Kirby and Whipple, 2001). Topography in the Siwalik Hills at this locality is developed above a fault-related fold in the frontal thrust of the Himalaya (Lavé and Avouac, 2000); spatial variations in the vertical velocity field associated with an approximately listric fault plane generate a pronounced asymmetry to the deformation field (Hurtrez et al., 1999). Because erosion rates apparently kept pace with differential rock uplift in this landscape (Lavé and Avouac, 2000), Kirby and Whipple (2001) argued that systematic differences in river profile shape that depend on the orientation of the channel to the rock uplift field reflect a simple adjustment of channel gradients to differential rock uplift. Subsequent analysis of colluvial channels (Lague and Davy, 2003), and of tributary channels (Koons and Kirby, 2007; Wobus et al., 2006a), confirmed a linear relation between channel steepness (k_{sn}) and incision rate. It seems likely that this relationship could reflect the combination of weak substrate (Lavé and Avouac, 2001) and extraordinarily high discharge during monsoon seasons (Bookhagen and Burbank, 2010), such that most flood events exceed any threshold for erosion of the channel bed. However, such a result remains no more than an inference at present. This example will be explored in more detail in the case study section below.

In the past decade advances in the measurement of catchment-mean erosion rates using cosmogenically-produced radionuclides, primarily ^{10}Be (Bierman and Steig, 1996; Brown et al., 1995; Granger et al., 1996) have opened a new direction in the study of channel adjustment to erosion rate. Rather than assume that channel incision rates keep pace with rock uplift, one can now measure erosion rates directly from ^{10}Be inventories in well mixed (e.g., Niemi et al., 2005), modern, sediment. Although the global dataset of such samples now numbers in the thousands (Portenga et al., 2011), we review here a selected subset of these studies that were carefully designed to explore the relationship between channel profiles and erosion rates.

The first of such studies was conducted by Safran et al. (2005) in the Bolivian Andes, who found a linear, if noisy, scaling relation between erosion rate and channel steepness across a wide range of erosion rates (Fig. 3). Relatively large scatter in these data may reflect differences in substrate lithology (Safran et al., 2005), high variability in erosion rates in the steep, rapidly eroding terrain (Niemi et al., 2005), non-equilibrium conditions within sampled catchments, noisy DEM data, or perhaps spatial variations in the amount of precipitation across the orographic front (Schlunegger et al., 2011). In contrast, more recent studies – in which channels were selected in advance to span a range of steepness values as well as to rule out any strong morphologic signatures of transient (i.e. non-equilibrium) conditions (see discussion in next section) – in eastern Tibet (Harkins et al., 2007; Ouimet et al., 2009), in the San Gabriel mountains of southern California (DiBiase et al., 2010), and in the Apennines of Italy (Cyr et al., 2010) all suggest various forms of a non-linear functional relationship similar in form to equation (12) (Fig. 3). Notably, the non-linear increase of channel steepness index (k_{sn}) with increasing erosion rate, as well as differences in the scaling from site to site (Fig. 3), appear to be consistent with the expectation from fluvial incision models that incorporate thresholds for incision (e.g., DiBiase and Whipple, 2011; Lague et al., 2005).

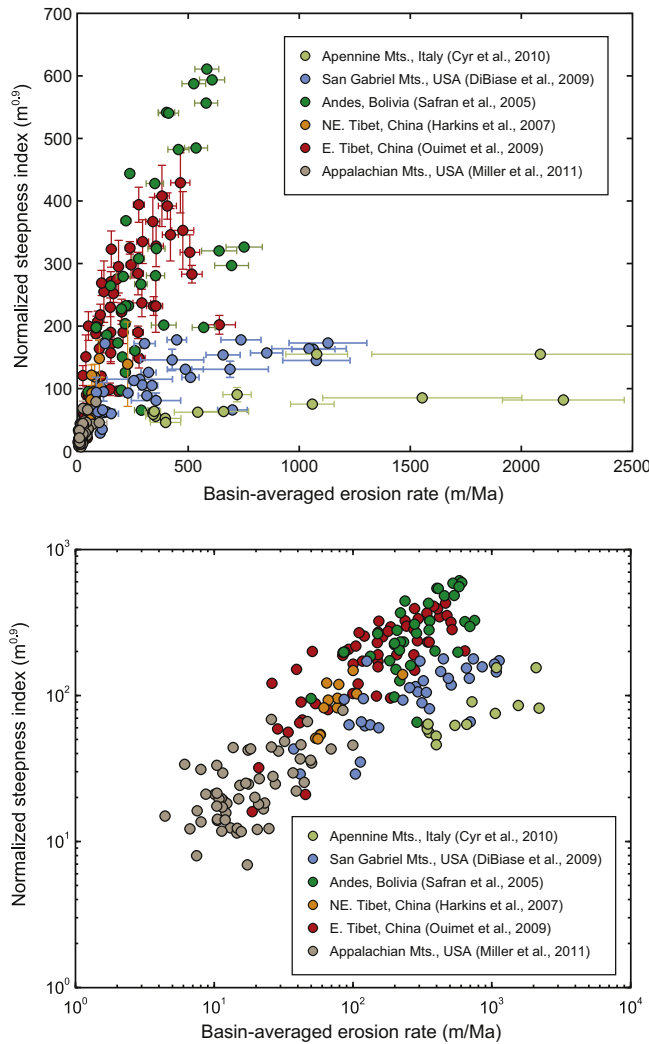


Fig. 3. Empirical scaling relationships between channel steepness (k_{sn}) and erosion rate from a variety of active orogens. In all examples, erosion rates were determined using the inventory of meteoric ^{10}Be in modern sediment and basins were selected such that channel profiles were likely to be in equilibrium with prevailing forcing (see text for discussion). For internal consistency, all erosion rate data were recalculated following Portenga et al. (2011). Original data sources are: Bolivian Andes (Safran et al., 2005), Eastern Tibet (Harkins et al., 2007; Ouimet et al., 2009), San Gabriel Mountains (DiBiase et al., 2010), Italy (Cyr et al., 2010), and Appalachians (Miller et al., 2011).

Comparison of the results of two studies in eastern Tibet (Harkins et al., 2007; Ouimet et al., 2009) highlights the potential utility of this approach. The two data sets were collected and processed by different research groups working within the eastern regions of the Tibetan Plateau, one in the deeply incised canyons draining into the Yangtze River (Ouimet et al., 2009) and one in the headwater reaches of the Yellow River (Harkins et al., 2007). Both data sets come from tributary catchments that are developed within flysch and greywacke of the Songpan-Ganzi terrane and thus sample rocks of similar strength, and precipitation is fairly uniform between the two regions ($\sim 0.3\text{--}0.5 \text{ m/yr}$, Ouimet et al., 2009). Importantly, both studies chose representative tributaries that exhibited a range of channel steepness indices, but took care to select only channels with smooth, graded profiles, suggestive of steady-state. Although the data of Harkins et al. (2007) sample a more limited range of channel steepness (Fig. 3), the near complete correspondence of these data with those of Ouimet et al. (2009) gives confidence that channel profiles in this region are indeed adjusted to match prevailing uplift rate patterns (c.f., Kirby and Ouimet, 2011).

Similarly, DiBiase et al. (2010) and Binnie et al. (2007) explored relationships between erosion rate and topography in the San Gabriel Mountains and adjacent San Bernardino Mountains, respectively. Their results are consistent with one another (DiBiase et al., 2010) and with independent longer-term erosion rate estimates (Spotila et al., 2002), despite sample collection by different researchers, sample processing in different labs, and AMS measurements taken in different facilities. Thus, despite inherent scatter in detrital cosmogenic erosion rate estimates (e.g., Matmon et al., 2003), there is rather remarkable reproducibility of general relationships between channel steepness and erosion rate.

Of course, significant uncertainties remain in extrapolating any single scaling to a more general understanding of the processes by which channels adjust morphology in response to increases in erosion rate. Lithology in some cases clearly influences channel steepness, as harder and less fractured rock is often associated with steeper channels (Duvall et al., 2004; Tressler, 2011). However, in other cases, differences in lithology have no discernable influence on the pattern of channel profiles (DiBiase et al., 2010; Kirby and Ouimet, 2011; Kirby et al., 2003; Ouimet et al., 2009). Possibly this reflects the prediction that where channels are blanketed by a thin veneer of alluvium, rock properties will have little influence on steady-state channel gradients except indirectly through bed material size (Sklar and Dietrich, 2006). Although some studies are consistent with this inference (e.g., Johnson et al., 2009a, b), the general problem of how rock mass strength quantitatively influences profile shape remains outstanding.

Likewise, although all channel incision models encode the expectation that wetter and/or stormier climates should lead to higher erosion rates (for a given channel steepness), at present there are only limited data that demonstrate this expected influence of climate on erosion rate unambiguously (see discussion by Aalto et al., 2006). Recent studies in the Central Andes (Bookhagen and Strecker, 2012) and along the North American – Central American Cordillera (Rossi et al., 2011) are consistent with this manner of response and suggest that further inquiry into the role of climate, particularly in relating regional mean climatology to event-scale dynamics, is warranted.

Despite these outstanding research questions, existing data provide compelling evidence that, within a given climatic setting, and subject to the caveat that rock strength may influence channel gradients, channel steepness indices of steady-state profiles represent a measure of relative variations in erosion and/or rock uplift rate consistent with a form similar to Equation (12). We are convinced that such studies now afford the possibility of developing semi-quantitative calibrations of the scaling between channel steepness (k_{sn}) and erosion rate that reflect the local combination of substrate erodibility and climate, and that such efforts can yield useful information about the rates and patterns of differential rock uplift (e.g., Kirby and Ouimet, 2011).

3.5. Transient channel response

Although the equilibrium profile of incising channels contains information regarding the combined effects of tectonics, lithology and climate, understanding the nature of channel response to perturbations away from such an equilibrium state is a critical aspect of any tectonic interpretation of river profiles. In this section, we show how the steady-state construct provides a basis for interpreting channel profiles undergoing a transient response to a change in climatic or tectonic forcing. A tectonic perturbation, such as development of a growing fold (e.g., Goode and Burbank, 2011), or a change in slip rate along an existing structure (e.g., Roberts and Michetti, 2004), engenders a change in relative baselevel (defined either locally, at the confluence with a higher order stream, an active

fault, or regionally as sea level), which, in turn, leads to adjustments in channel form (e.g., Howard, 1994; Whipple and Tucker, 2002, 1999; Whittaker et al., 2007a). The duration over which the landscape responds to such a change in forcing is dependent on the physical scale of the system, the nature of the perturbation, and the erosional efficiency of the fluvial system (e.g., Attal et al., 2011; Whipple, 2001). Here, we use the term “efficiency” to refer to the aggregate suite of factors that govern how readily a river is able to remove mass, both intact bedrock and sediment load, along a given reach (often encapsulated as K , Equation (10b)). Typically, response timescales in active orogens range from 10^4 to 10^6 years (Baldwin et al., 2003); as such, the transient response to changes in tectonic forcing encodes a signal of time-varying deformation integrated over multiple seismic cycles (e.g., Hiley and Arrowsmith, 2008).

The degree to which fluvial systems record temporal variations in deformation, of course, also depends on the nature and spatial extent of the forcing. Forcing may be a discrete event, such as stream capture or fault rupture, that generates a temporary deviation away from an initial condition. Persistent forcing, such as a sustained change in slip rate along a fault system, in contrast, will drive the fluvial system toward a new equilibrium condition (Bonnet and Crave, 2003; Tucker and Whipple, 2002). The response to cyclic forcing, such as may be driven by long-term shifts in climate state, depends on the period of the forcing relative to the response time; if forcing is short relative to the response time, the system will approximate a steady-state around the mean (Snyder et al., 2002). If, however, the forcing is long, the system will oscillate between two stable end-member equilibrium states (Stolar et al., 2006; Whipple and Tucker, 2002). The spatial pattern of forcing (generally, the differential rock uplift associated with fault slip and/or fold growth) also influences the manner of response; systems tied to local baselevel across a range-front fault tend to behave in a relatively simple manner, as the pattern of rock uplift is driven largely by fault slip (e.g., Attal et al., 2011, 2008; Densmore et al., 2003; Densmore et al., 2004; Whittaker and Boulton, 2012; Whittaker et al., 2007b), whereas those developed across a growing fold depend strongly on the kinematics of fold growth and the consequent pattern of differential rock uplift along the fold limbs (e.g., Goode and Burbank, 2011; Molnar, 1987).

A final set of complexities arise because we expect that changes in climate can alter the efficiency of fluvial incision (Bonnet and Crave, 2003; Turowski et al., 2007). Perturbations in climate thus may also drive changes in river profile form, the morphology of which can in principle be identical to that of a tectonic forcing (e.g., Whipple, 2001, 2009). Consequently any tectonic interpretation of river profiles requires due consideration of this possibility. Additionally, it is important to note that either formation of fluvial hanging valleys due to non-linearities in transient river response (Crosby et al., 2007; Goode and Burbank, 2009; Wobus et al., 2006b) or feedbacks between channel incision and sediment delivery from hillslopes may prolong the response times of the system (e.g., Korup et al., 2010; Ouimet et al., 2007).

With these caveats in mind, we approach the question of how fluvial systems respond to a perturbation in tectonic forcing. We follow Whipple (2001) in distinguishing between “rising state” transients, in which the change in forcing engenders a response that drives an increase in the efficiency of fluvial incision (i.e., an increase in differential rock uplift rate and/or a shift to more erosive climate state) and “declining state” transients, in which the system is driven toward a less erosive condition (Baldwin et al., 2003). In both cases, the system response is associated with the generation and migration of knickpoints – discreet changes in the steepness of the river profile – whose form and behavior depend on both the nature of the perturbation and the mechanics of river incision. We first briefly discuss knickpoint evolution, and then consider their interpretation as a means to distinguishing spatial from temporal effects in landscapes.

3.5.1. Knickpoints in erosive landscapes

As discussed by Whipple et al. (2011), knickpoints in erosive river systems that develop in response to a perturbation can be considered as the migrating boundary between downstream regions that are adjusting to the new forcing and upstream regions that retain characteristics of the pre-existing, or background, state (e.g., Crosby and Whipple, 2006; Howard et al., 1994). As first discussed by Haviv et al. (2010), knickpoints can be grouped into two end-member morphologies: vertical-step knickpoints and slope-break knickpoints (Fig. 4). Both morphologies are marked by

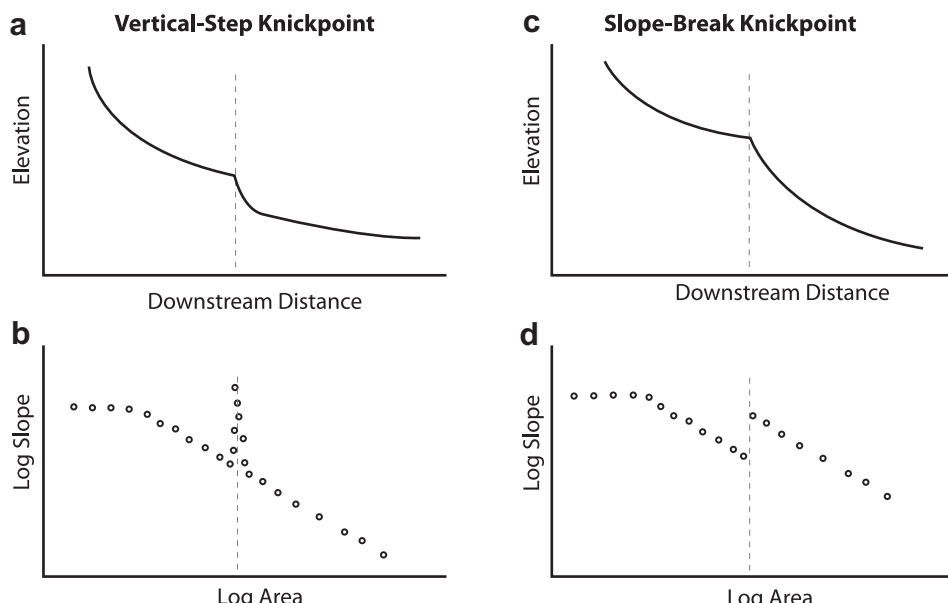


Fig. 4. Classification of knickpoints in terms of both channel profile and slope-area scaling relationships. Both morphologies may be either mobile, representing a transient perturbation to the fluvial system, or anchored in place by resistant substrate, landslide debris, or active faults. Figure modified from Whipple et al. (2011).

distinctive changes in channel gradient and thus may be recognized on slope-area or slope-distance plots (Goldrick and Bishop, 2007; Wobus et al., 2006a). Although both types of knickpoints may evolve as either mobile features that migrate through a drainage network or as fixed features, anchored in space, in our experience a great majority of vertical-step knickpoints tend to be spatially associated with discrete heterogeneities along the profile. Spatial correlations of steepened channel segments with coarse debris from landslides (Korup, 2006), debris-flows at tributary junctions and/or locally resistant substrate (e.g., Kirby et al., 2003) suggest that these are often anchored in space. Thus, small (relative to catchment relief), discrete vertical-step knickpoints often have no direct tectonic significance beyond the general observation that landslides tend to be more common in rapidly uplifting regions (e.g., Korup et al., 2010). Distinguishing fixed knickpoints from mobile ones typically requires corroborating information, such as the direct correlation between rock strength and channel gradient (e.g., Duvall et al., 2004) or incision rate patterns suggesting passage of an incisional wave (Reusser et al., 2004; Seidl and Dietrich, 1992). The interested reader is referred to Whipple et al. (2011) for a more thorough discussion of knickpoint morphology and behavior.

In contrast to vertical-step knickpoints, those that represent a break in slope-area scaling (Fig. 4) typically develop in response to a persistent change in forcing, either spatial or temporal. Consequently, slope-break knickpoints play a central role in the interpretation of tectonics in erosional landscapes (Wobus et al., 2006a). Because these knickpoints sweep upstream at predictable rates (Attal et al., 2008; Bishop et al., 2005; Crosby and Whipple, 2006; Rosenbloom and Anderson, 1994), their spatial distribution can be expected to form systematic patterns that serve to guide interpretation (e.g., Berlin and Anderson, 2007; Goldrick and Bishop, 2007; Harkins et al., 2007; Wobus et al., 2006a). Identification of such slope-break knickpoints arrayed linearly across the landscape in channels of different sizes and orientations, and corroborated by measurements of differential rates of erosion, have led to identification of previously unrecognized, active structures in the Nepalese Himalaya (Wobus et al., 2005, 2003) and eastern margin of the Tibetan Plateau (Kirby and Ouimet, 2011; Kirby et al., 2003). These examples are developed further below in the section on case studies.

3.5.2. Tectonic interpretation of transient profiles

Transient river profiles have now been recognized in tectonically active landscapes around the globe and have been used to infer changes in rock uplift rate along the Red River fault in SE China (Schoenbohm et al., 2004), in the Sierra Nevada and San Gabriel mountains of California (Clark et al., 2005; Wobus et al., 2006a), adjacent to the San Andreas fault in northern California (Johnson et al., 2009a, b; Kirby et al., 2007), within the San Jacinto fault zone in southern California (Dorsey and Roering, 2006), along the western margin of the central Andean plateau (Hoke et al., 2007), and in the Argentine Precordillera (Walcek and Hoke, 2012). Similarly, transient river profiles have been central in the study of landscape response to baselevel fall in the Waipaoa river in New Zealand (Crosby and Whipple, 2006), in coastal Scotland (Bishop et al., 2005), in the Apennines of central Italy (Attal et al., 2011, 2008; Whittaker et al., 2008; Whittaker and Boulton, 2012; Whittaker et al., 2007a, b), along the Colorado River in the western US (Berlin and Anderson, 2007; Cook et al., 2009), along the Yellow River in northeastern Tibet (Harkins et al., 2007), and in a small catchment in Spain (Reinhardt et al., 2007). Moreover, a number of recent studies in active orogens around the globe use the distribution of knickpoints to argue for recent changes in tectonic forcing, along core complexes in the Woodlark Basin (Miller et al.,

2012), along the southern margin of the central Anatolian plateau (Schildgen et al., 2012), within the Cordillera de Talamanca of Costa Rica (Morell et al., 2012), in the Sila Massif of southern Italy (Olivetti et al., 2012), and in eastern California (see case study below). Most of these observations, and the inferences drawn from them, rely on a conceptual model of how slope-break knickpoints evolve in fluvial systems. In this section, we review the assumptions underlying these inferences, and discuss how one can reconstruct the magnitude, and in some cases, the rate of differential rock uplift recorded by transient channel profiles.

It is well-known that most of the stream-power family of models described previously predict that the leading edge of a transient response to a change in the uplift rate of rock will migrate upstream as a kinematic wave (Rosenbloom and Anderson, 1994), where the celerity is a function of contributing drainage area (Crosby and Whipple, 2006; Whipple et al., 1999). This leads directly to a strong dependence of the map-view knickpoint migration rate on the size of upstream watersheds (e.g., Bishop et al., 2005). However, Niemann et al. (2001) showed that slope-break knickpoints migrate at a constant vertical rate, under two simplifying assumptions. First, equilibrium channel profiles must be well-described by a slope-area scaling relationship like that in Equation (1), where the steepness index (k_s) depends on the rock uplift rate but the concavity index (θ) does not. Note this is consistent with the observations from equilibrium landscapes described previously and from the recognition that many river profiles consist of multiple segments with similar concavity but distinct channel steepness (e.g., Wobus et al., 2006a). Second, the transient response is characterized by slope-break knickpoints that separate reaches that are in equilibrium with previous conditions (above the knickpoint) and the current conditions (below the knickpoint). Under these assumptions, knickpoints associated with a sustained change in rock uplift rate should lie at a uniform elevation above baselevel. Although such patterns have been recognized in a number of landscapes (e.g., Cook et al., 2009; Wobus et al., 2006a), any deviation from the idealized response will lead to a dispersion of knickpoint elevations. Likewise, spatial variations in upstream channel form, perhaps reflecting non-uniform background rates of rock uplift (e.g., Harkins et al., 2007) may lead to systematic variations in knickpoint elevation.

Although changes in tectonic forcing appear to be the driver of many slope-break knickpoints, it is also possible that climate changes engender a similar response. In particular, if the rate of differential rock uplift remains constant, but the erosional efficiency of fluvial systems is reduced (perhaps associated with a pronounced shift in climate state), channel systems will be forced to steepen until erosion is once again able to balance rock uplift (Bonnet and Crave, 2003; Whipple, 2001). Under the assumptions noted above, the behavior of fluvial systems in response to such a change in forcing will be nearly identical to a change in rock uplift. As such, distinguishing between a tectonic and climatic signal may be difficult.

3.5.3. Reconstruction of channel profiles

One of the potentially powerful implications of interpreting transient slope-break knickpoints is that it allows for reconstruction of the “relict” channel profile. Under the assumption that the reach of the channel upstream of the knickpoint was equilibrated to a previous set of conditions, one can generate a model estimate of the shape of the profile using the scaling relationship between channel slope and drainage area (Equation (1)). By projecting this scaling out to the mountain front (or, alternatively, to the position of the fault inferred to be responsible for setting the uplift rate boundary condition), one can estimate the former shape of the profile via simple integration of Equation (1). Moreover, combining

uncertainties determined on channel steepness (k_{sn}) from the integral approach (Equation (7)) with uncertainties in knickpoint elevation (Harkins et al., 2007), one can develop reasonable estimates of uncertainty in the shape of the reconstructed profile (Walcek and Hoke, 2012). Provided that upstream reaches are not subject to long-wavelength tilting, the difference in elevation between the present-day elevation at the range front and the reconstructed elevation places a minimum constraint on the magnitude of differential rock uplift since the onset of the transient. Such an approach was first used to estimate the amount of surface uplift associated with the southeastern most portions of the Tibetan Plateau, along the Red River fault zone (Schoenbohm et al., 2004), and has subsequently been used in the Sierra Nevada (Clark et al., 2005), along the Yellow River in northeastern Tibet (Harkins et al., 2007), along the flanks of the Chilean (Hoke et al., 2007) and Bolivian (Barke and Lamb, 2006) Andes, and along tributaries of the Colorado River (Berlin and Anderson, 2007; Cook et al., 2009).

It is important to note, however, that reconstruction of the relict profile provides only a minimum estimate of the total amount of incision and/or rock uplift (Fig. 5), because the upstream, relict channel segment continues to lower at the rate to which it was previously adjusted. If this rate is high and/or the duration of the transient is long, the amount of lowering could be a significant and should be included in any interpretation. The difficulty of measuring both the rates of channel lowering and the duration of transient conditions, however, makes a definitive assessment of the magnitude of incision difficult. To our knowledge, this has only been done well in a limited number of studies, all of which rely on ancillary information regarding the rates and/or magnitude of incision both above and below knickpoints (Harkins et al., 2007; Schildgen et al., 2012; Schoenbohm et al., 2004). In northeastern Tibet, the Yellow River is incised into a deep canyon as it crosses a broad region of high topography in the Anyemaqen Shan. Harkins et al. (2007) analyzed tributaries to the main Yellow trunk stream, all of which had pronounced knickpoints along their lower reaches. A combination of systematic variations in knickpoint elevation and reconstruction of relict profiles allowed these authors to estimate the former shape of the trunk profile. Moreover, erosion rates determined from inventories of cosmogenic ^{10}Be from watersheds

above knickpoints provided a measure of the co-variance of erosion rates and channel steepness (k_{sn}) in the relict landscape, while dating of fluvial terraces along the trunk stream provided an estimate of the timing of onset of incision. Collectively, this approach allowed these authors to quantitatively estimate both the magnitude of transient incision associated with migratory knickpoints, as well as the amount of lowering within the relict, quasi-equilibrium landscape (Harkins et al., 2007).

4. Case studies

The relationship between differential rock uplift rate and steady-state channel steepness and the transient response to changes in differential rock uplift allow interpretation of both spatial and temporal patterns in active deformation. At first glance, the challenge of inferring tectonic history from geomorphic observations seems insurmountable given the complexities inherent in the systems. It is important to emphasize that the quantitative relationship between channel steepness and rock uplift rate is not yet fully understood and may be different under steady and transient forcing (Whipple, 2004), perhaps because of additional adjustments in channel hydraulic geometry (Finnegan et al., 2005; Stark, 2006; Wobus et al., 2006c, 2006d) and percent rock exposure in the channel bed (Sklar and Dietrich, 2004, 2006; Turowski et al., 2007) during transient periods of rapid incision. Likewise, in regions with pronounced variations in climate and/or strong orographic forcing of precipitation, one needs to take care to account for the influence of variations in discharge on the relationship between channel profile form and erosion rate (Bookhagen and Burbank, 2010). Finally, local perturbations to river profiles such as landslides (Korup, 2006; Ouimet et al., 2007), lithologic properties (Duvall et al., 2004), and simple artifacts in DEMs can add noise to any individual profile (Wobus et al., 2006a).

Despite these complexities, much can be inferred from analysis of topography, provided one approaches the question as a series of multiple working hypotheses. In our experience, two aspects to successfully determining whether spatial variations in channel steepness are attributable to tectonic, climatic, or lithologic influences in space and time are: (1) the systematic analysis of channels

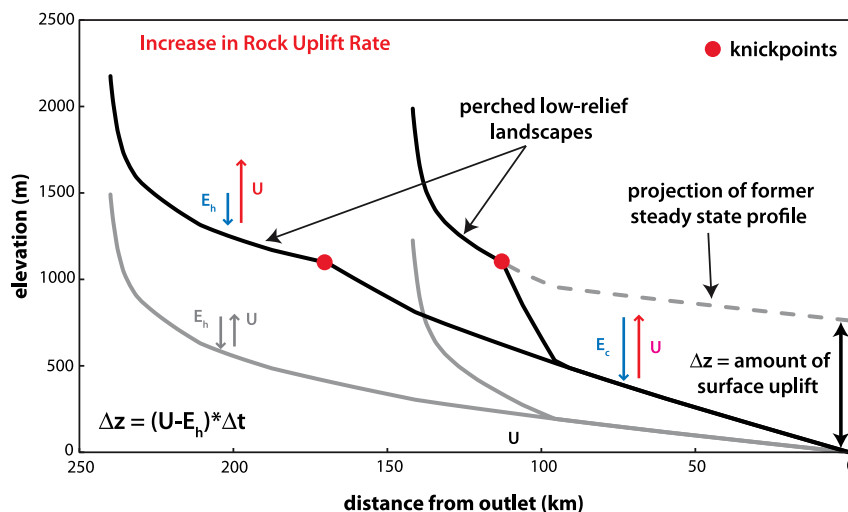


Fig. 5. Cartoon showing the process of forming and removing a transient landscape. Grey lines depict the original form of a well adjusted, steady-state river profile with one tributary. The black lines show the form of the same fluvial system that has experienced an increase in rock uplift rate (U). The river first adjusts to the new erosion rate (E_c) closest to the outlet and then a wave of higher erosion rate propagates headward. Because the upper reaches of the river continued to erode at the previous erosion rate (E_h), they maintain their original form. This dichotomy in erosion rate, and thus form, creates a knickpoint in the river profile. Since the vertical knickpoint velocity is constant (Niemann et al., 2001), we find knickpoints at the similar elevations within the fluvial system. Once the wave of incision has propagated through the network, the entire fluvial system will return to a steady-state at a higher erosion rate than before. Under these conditions, the projection of the relict profile out to the mountain front provides a measure of surface uplift.

of varying size, orientation (e.g., Kirby and Whipple, 2001) and landscape position, and (2) the examination of multiple landscape metrics in concert, including local relief and hillslope gradient (Gabet et al., 2004) in addition to channel steepness patterns. Such a combined approach affords the best opportunity to reveal patterns in the landscape that are diagnostic of temporal or spatial forcings, and patterns that indicate strong associations with lithologic boundaries, active faults, and/or climatic gradients. Although it is probably not possible to define a complete set of guidelines for how to differentiate among all possibilities that may be encountered in different landscapes, we illustrate below, and in our previous work, how the general principles outlined above can be employed in tectonic interpretations. Although topographic data alone will always be multiply interpretable and one must be ever mindful of the many remaining uncertainties in river response to tectonics, climate and lithology (noted above), thoughtful application of stream-profile analysis can be a powerful reconnaissance tool with which to interrogate the rates and patterns of deformation in active mountain belts.

4.1. Case Study I – steady-state landscapes in the Siwalik Hills

Growing folds in the foothill ranges of the Nepalese Himalaya present an excellent example of channel adjustment to tectonic forcing in a steady-state landscape. Differential rock uplift across a fault-bend fold is associated with slip along the Main Frontal Thrust, the primary structure accommodating convergence between India and southern Tibet (Lavé and Avouac, 2000, 2001). In a landmark study, Lavé and Avouac (2000) used deformed fluvial terraces along two transverse rivers crossing the anticline to reconstruct the pattern and rates of fluvial incision. They were able to show that 1) rates of incision varied in space, but were steady throughout the Holocene, and 2) that the pattern of incision matched the long-term pattern of deformation recorded in folded strata of the Siwalik group. Notably, the geometry of the MFT in central Nepal appears to vary smoothly with depth, such that the vertical component of the rock velocity field varies from a few mm/yr north of the fold to nearly 15 mm/yr along the fold crest (Lavé and Avouac, 2000).

These spatial variations in rock uplift rate, coupled with the high rates of precipitation along the Himalaya (Bookhagen and Burbank, 2010), relatively homogeneous, weak bedrock (sandstones and mudstones) of the Lower and Middle Siwaliks (Lavé and Avouac, 2001), and steady incision present a nearly ideal field site to explore the steady-state variations in topography with uplift/erosion rate. Hurtrez et al. (1999) demonstrated a correlation between local relief (measured over lengthscales <700 m) and uplift rate. Kirby and Whipple (2001) showed that fluvial channels developed along the flanks of the range exhibited systematic patterns of channel concavity and steepness that correlated with the pattern of differential rock uplift (see below). Lague and Davy (2003) examined colluvial channels (developed at drainage areas <1 km²) and found a near linear correspondence between colluvial channel steepness and uplift rate. Thus, all measures of topography above these growing folds suggest that channel gradients are adjusted to match spatially variable rock uplift (Miller et al., 2007).

We have subsequently updated the analysis of Kirby and Whipple (2001) on this range by using a higher-resolution DEM, generated from the ASTER instrument. We interpolate uplift rates using the raw terrace data of Lavé and Avouac (2000), essentially assuming that fault dip varies smoothly between the two transects. This approach eliminates some of the along-strike variability in uplift rates seen in the studies of Hurtrez et al. (1999) and Lague and Davy (2003). The results of our analysis of the 30 m ASTER DEM confirm previous work (Kirby and Whipple, 2001) in that

three categories of channels emerge: 1) those crossing from the locus of high uplift along the crest of the range toward the flanks exhibit high concavities, 2) channels parallel to the fold axis (and thus parallel to gradients in rock uplift) exhibit concavities in the range of ~0.5 (Fig. 6a), consistent with the expectation for steady-state channels developed against spatially invariant uplift, and 3) rivers crossing the fold from north to south exhibit convex profiles (Fig. 6a). Although Kirby and Whipple (2001) couched their analysis in the language of the stream-power incision model, it is important to note that these observations are independent of any such choice.

This point is further emphasized by careful examination of channels developed parallel to the fold axis. Despite little variation in channel concavity (Kirby and Whipple, 2001), these channels exhibit systematic variations in channel steepness index (k_{sn}) that suggest a linear adjustment to the local rate of rock uplift (Fig. 6b). Fortunately, most of these channels are of similar size, and so are appropriate for use of a reference slope (S_r) metric also (Sklar and Dietrich, 1998). Comparison of the two methods provides a compelling argument that this result is robust (Fig. 6b). Notably the downstream increase in gradient along the transverse rivers nearly matches the difference in gradients along strike-parallel streams (Fig. 6a), suggesting that the adjustment of fluvial systems of varying orientation is of the same degree, and it is this adjustment that appears to be responsible for the convex-upward profiles utilized by Kirby and Whipple (2001) to argue for a simple incision rule.

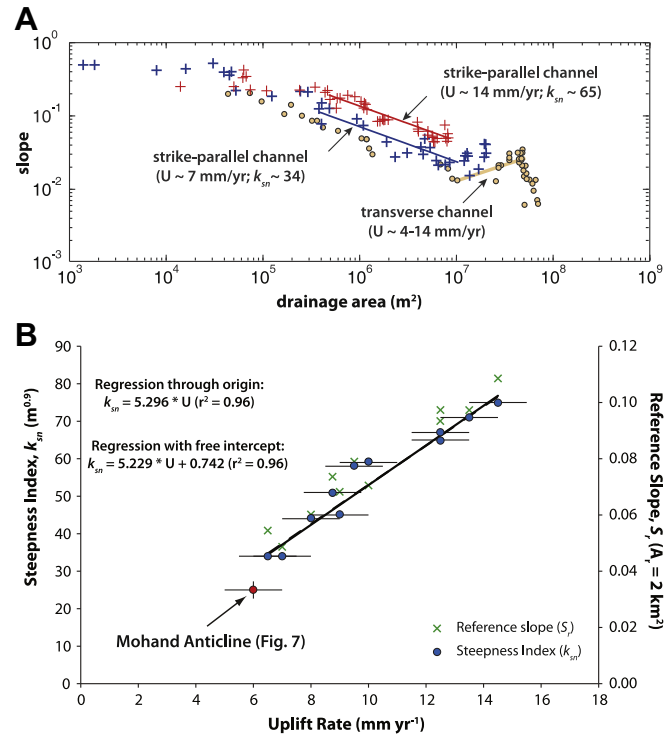


Fig. 6. Results of channel steepness analysis in the Siwalik Hills of Central Nepal. A.) Comparison of slope-area data for three channels extracted from ASTER 30m DEM. Channels in blue and red are developed parallel to the fold axis and are experiencing approximately uniform rock uplift rates along their length (blue = ~7 mm/yr; red = ~14 mm/yr). Rates are inferred from data of Lavé and Avouac (Lavé and Avouac, 2000). Note that both have similar concavities, but channels at higher uplift rate are steeper. B.) Channel steepness (blue) for 11 drainages parallel to fold axis; k_{sn} varies approximately linearly with uplift rate in this landscape. Green crosses represent the reference slope, an alternative measure of channel steepness (Sklar and Dietrich, 1998). Red point represents the mean of channel steepness indices determined for 14 channels on the southern flank of the Mohand Anticline in northwestern India (see Fig. 7).

To test whether this empirical relationship between channel steepness and rock uplift rate has predictive power elsewhere in the Himalayan foreland, we conducted a new analysis of channels developed along the southern flank of the Mohand anticline, near Dehra Dun, India (Fig. 7a), approximately 600 km northwest of central Nepal. The Mohand anticline appears to be a typical fault-bend fold (Powers et al., 1998; Wesnousky et al., 1999) developed above a ramp in the Main Frontal Thrust (MFT) dipping at $\sim 30^\circ$ (Fig. 7b). A relatively precise reconstruction of surface dip data led Mishra and Mukhopadhyay (2002) to model the fold as developing above a fault plane with two, slight synformal bends (Medwedeff and Suppe, 1997) and $\sim 4\text{--}5$ km of shortening. The consequence of this geometry is that, in contrast to the strong spatial variations in rock uplift in central Nepal (Lavé and Avouac, 2000), rock uplift rates are expected to be relatively uniform across the fold. A single fluvial terrace, dated with radiocarbon by Wesnousky et al. (1999), constrains both the minimum vertical incision rate (6.9 ± 1.8 mm/yr) and the slip rate along the fault (13.8 ± 3.6 mm/yr).

Analysis of channel profiles of 14 rivers developed along the southern flank of the Mohand anticline reveal the presence of subtle, slope-break knickpoints in most river profiles

(Fig. 7a; Fig. 8a). Channel segments upstream of knickpoints exhibit relatively uniform concavities (mean of 0.46 ± 0.11 , Fig. 8b) and channel steepness indices (mean k_{sn} of 15.1 ± 2.9 , Fig. 8b) in contrast, lower channel segments are steeper (mean k_{sn} of 25.1 ± 2.3 , Fig. 8b) and exhibit a wider range of concavity (mean of 0.52 ± 0.4 , Fig. 8b) that likely reflects a transition to alluvial conditions as uplift rates go to zero across the trace of the MFT. Although these knickpoints could reflect 1) a temporal increase in uplift/incision rates along the entire fault system, 2) spatial differences in uplift rate localized along a kink band in the fault-bend fold, or 3) lithologic differences between strata within the Siwaliks Group, we favor the last interpretation for the following reasons. First, knickpoints appear to be localized along the mapped boundary between the Upper Siwaliks and the Lower Middle Siwaliks (Barnes et al., 2011; Raiverman et al., 1990; Wesnousky et al., 1999), and the poorly consolidated nature of the Upper Siwaliks is consistent with a weaker substrate (leading to lower k_{sn}). Second, there is no evidence for strong spatial gradients in rock uplift; the kink band axis implied by the fold geometry (Mishra and Mukhopadhyay, 2002) projects east of the crest of the range (Fig. 7b), implying that rock uplift rates should be nearly uniform along the southern flank of the range. Third, although it is

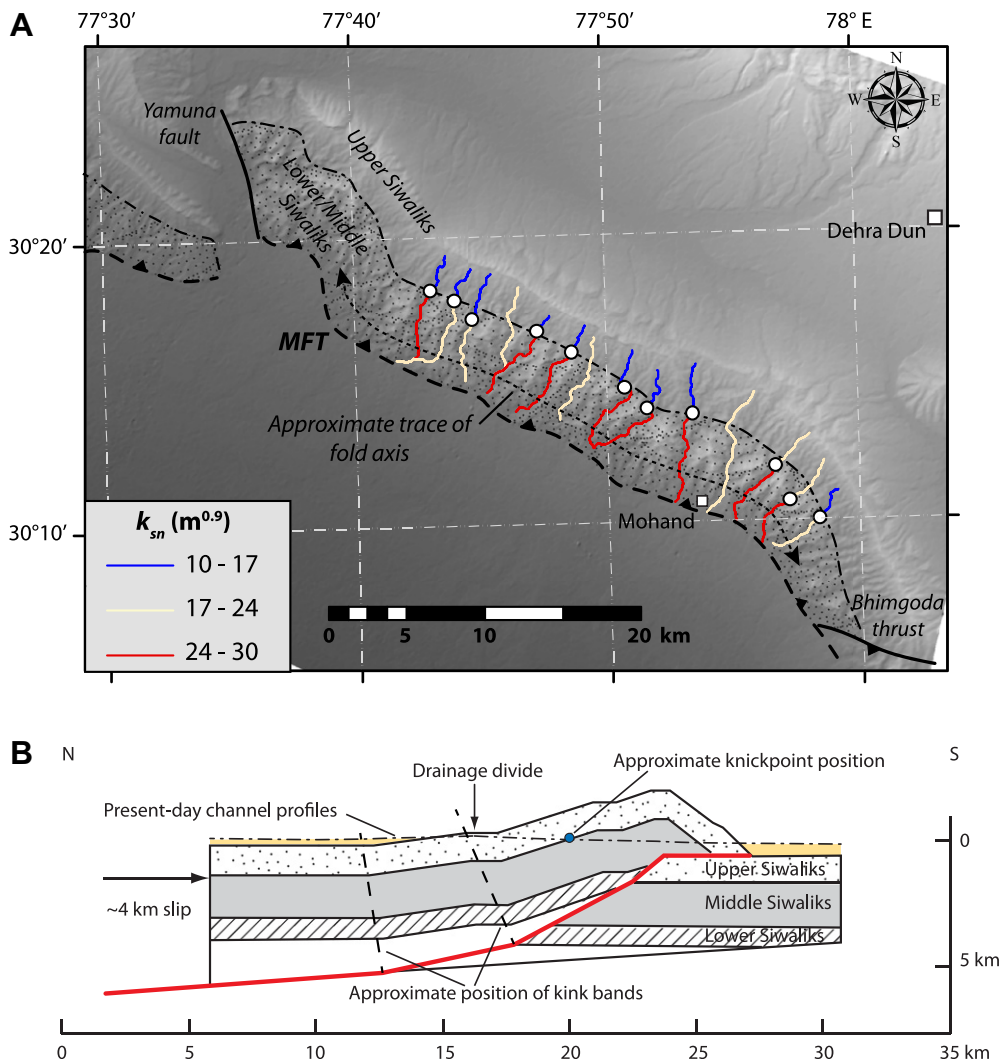


Fig. 7. Analysis of channel profiles along the flank of the Mohand Anticline, in northwestern India. A.) Shaded-relief map with channels color-coded by steepness index. Knickpoints are shown as white circles and correspond closely with the transition from Upper to Middle Siwaliks. Geology after Wesnousky et al. (1999). B.) Balanced cross-section across the Mohand anticline, modified after Mishra and Mukhopadhyay (2002) and Barnes et al. (2011).

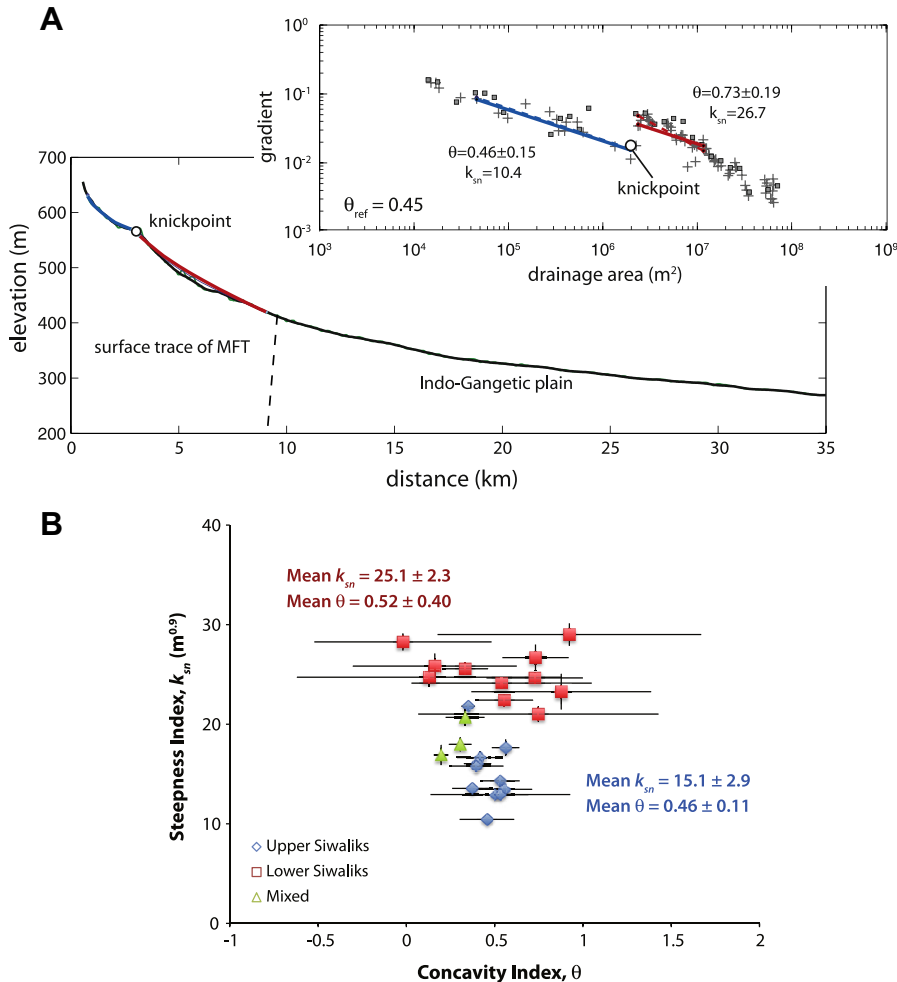


Fig. 8. Results of channel profile analysis along the Mohand anticline. A.) Example profile and slope-area data (inset) showing break in scaling that separates profile into two segments interpreted to reflect differences in substrate erodibility (see text for details). B.) Variability of channel steepness (k_{sn}) and concavity (θ) for channel segments upstream (blue) and downstream (red) of knickpoints.

more difficult to rule out the possibility of a recent increase in fault slip rate, the relative maturity of the fault-fold system, with 4–5 km of slip, makes this possibility less likely.

Comparison of these results, with the scaling of channel steepness (k_{sn}) and rock uplift rate from Central Nepal (Fig. 6b) suggests that this empirical scaling may hold along much of the Himalayan foreland. When we directly compare channel steepness in the Lower and Middle Siwaliks, the Mohand anticline falls along the predicted trend (Fig. 6b). Or, to turn this analysis around, if we take the channel profiles along the southern flank of the Mohand anticline, and predict erosion rates using the empirical scaling from Nepal, we find that predicted erosion rates range from 7 to 8 mm/yr, nearly exactly the rates measured by Wesnousky et al. (1999). To our thinking, this result illustrates the potential of stream profile analyses to predict patterns (and possibly, rates) of erosion along growing structures. In so far as those rates are adjusted to match rock uplift driven by deformation, they provide a new avenue into mapping deformation rates on foreland fault systems.

4.2. Case study II – geomorphic fingerprints of active deformation in the Himalaya and Tibet

The structural and tectonic implications of the transition from the physiographic Lesser to Higher Himalaya (Fig. 9) has been

debated at least since Seeber and Gornitz (1983) first noted that oversteepened reaches of major trans-Himalayan rivers coincide with a belt of seismicity along the Himalayan arc in the vicinity of the Main Central Thrust (MCT). This debate has intensified in the past decade, fueled by a combination of geomorphic analysis of ~90 m resolution digital elevation models (DEMs), thermochronometry, and thermal-kinematic modeling.

The most widely held interpretation has been that this physiographic transition (Fig. 9) and cluster of seismicity reflects transport of the upper plate over a crustal ramp in the basal thrust that breaks the surface as the Main Frontal Thrust (MFT) ~100 km to the south (Fig. 10a). The cluster of seismicity is thought to be related to slip and strain accumulation on the ramp; only great earthquakes (magnitude >8) are thought to rupture the locked décollement under the Lesser- and Sub-Himalaya (e.g., Avouac, 2003; Bilham et al., 1997; Cattin and Avouac, 2000; Meade, 2010; Ni and Barazangi, 1984; Pandey et al., 1995; Seeber and Armbruster, 1981). In this interpretation deformation is largely in sequence and the MCT is a defunct Miocene structure that only coincidentally outcrops in the vicinity of the sub-surface ramp.

Geomorphic and thermochronologic evidence, however, indicates that this model is incomplete and at least in part incorrect. Wobus et al. (2003; 2006d) have demonstrated that in central Nepal this physiographic transition is very sharply defined and

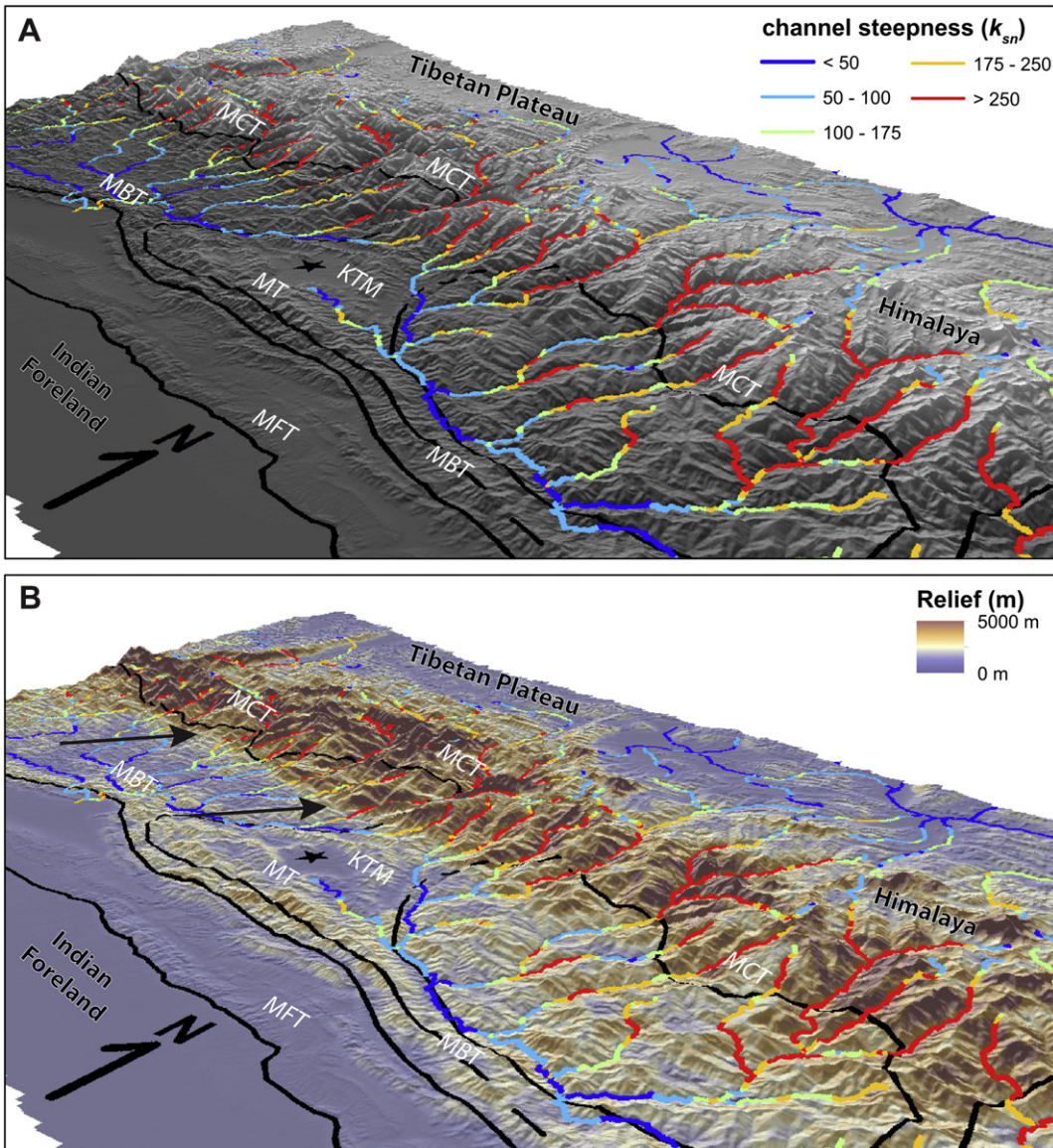


Fig. 9. Perspective views of topography, local relief, and channel steepness patterns in the Himalaya of central Nepal (KTM: Kathmandu; 1.5× vertical exaggeration). Major thrusts labeled on hanging wall: Main Central Thrust (MCT), Mahabarat Thrust (MT), Main Boundary Thrust (MBT) and Main Frontal Thrust (MFT). A. Topography and channel steepness index ($\theta_{ref} = 0.45$). B. Topography color-coded by local relief within 2.5 km radius (reds = high, blues = low). Note the abrupt, linear physiographic transition between the Lesser and Higher Himalaya (arrows) associated with a step-function increase northward in mean elevation, local relief, and channel steepness. (For interpretation of the references to colour in this figure legend, the reader is referred to the web version of this article.)

remarkably linear for over 300 km along strike (Fig. 9). Here the physiographic transition has all the geomorphic attributes expected for an active out of sequence thrust fault in the approximate tectono-stratigraphic position of the MCT: an abrupt, collinear, northward increase in mean elevation, hillslope gradient, local relief, and channel steepness associated with an increase in erosion rate and a decrease in soil cover and weathering extent on hillsides and an increase in bedrock exposure in channel bed and banks (Wobus et al., 2005, 2003, 2006d). Analysis of channels of different size, orientation, and position relative to changes in mean elevation, local relief, hillslope gradients, lithologic contacts, and the physiographic transition with the associated increase in orographic rainfall (e.g., Bookhagen and Burbank, 2006) was critical in isolating the tectonic signal and determining how abruptly rock uplift rate must increase to the north (Wobus et al., 2003, 2006d).

Although these attributes are suggestive of a surface-breaking thrust, they are ultimately only diagnostic of an abrupt increase in rock uplift rate at the physiographic transition. Such a break in rock uplift rate could be accommodated by a sharply defined fold at the surface associated with a thrust ramp or growing duplex at depth. Of the three plausible interpretations of deformation patterns associated with the physiographic transition (Fig. 10), only the first, traditional interpretation of simple transport over a crustal ramp can be ruled out as incompatible with the thermochronologic data (Wobus et al., 2006d). Several researchers have demonstrated that active duplex formation associated with accretion of Lesser Himalayan rocks across the ramp (Fig. 10b) can explain both the geology and thermochronologic data from a transect across the Kathmandu Klippe (Avouac, 2003; Bollinger et al., 2004, 2006; Herman et al., 2010; Robert et al., 2009). Although the abrupt, linear nature of the physiographic transition (Fig. 9) and the exact

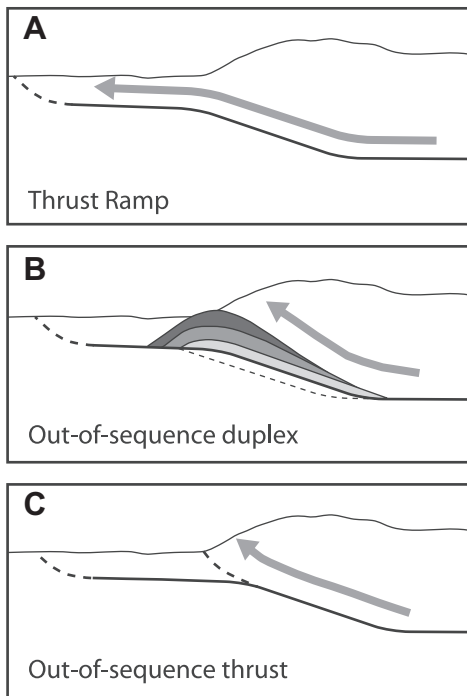


Fig. 10. Schematic cartoon cross-section illustration of published alternate interpretations of the deformation patterns responsible for the uplift of the High Himalaya. A. Transport over a ramp in the basal thrust. B. Out of sequence duplex formation associated with underplating of Lesser Himalayan rocks across the ramp. C. Out of sequence thrust splaying off the underlying ramp. Figure modified after Wobus et al. (2006d).

coincidence of breaks in mean elevation, local relief, channel steepness, erosion rates, and $^{40}\text{Ar}/^{39}\text{Ar}$ cooling ages were not directly addressed in these papers. Wobus et al. (2006d) showed that under a narrow range of conditions duplex growth associated with accretion across the ramp (Fig. 10b) can indeed explain all observations.

Despite the debate over structural architecture and internal deformation patterns of the Nepalese Himalaya, the geomorphic interpretation that an abrupt increase in rock uplift rate is responsible for the physiographic transition (Fig. 9) is not disputed. Indeed, the increase in rock uplift rate required to explain the increase in local relief and channel steepness is amplified by the ~4-fold increase in orographically induced rainfall on the flanks of the High Himalaya (Bookhagen and Burbank, 2006, 2010) that is expected to increase erosion rates for a given topography (Equation (10)). Moreover, regardless of whether the physiographic transition reflects a surface-breaking thrust fault or the growth of a duplex at depth, both scenarios involve significant out of sequence deformation that could be influenced by climatically controlled erosion patterns and that play a key role in mountain building. Why this locus of rock uplift and deformation has been so long-lived at this location, in the vicinity of the MCT, is a key, unresolved issue in Himalayan tectonics.

Despite the inherent limitation that geomorphic analyses may reveal rock uplift patterns but may not be diagnostic of the underlying structural configurations, work elsewhere in the Himalaya and Tibet demonstrates the potential for study of landscape morphology to identify active faults. Kirby et al. (2003) identified an analogous, abrupt physiographic transition at the foot of the Longmen Shan in China's Sichuan province. Based on largely morphologic evidence, Kirby et al. (2003) suggested that the Yingxiu-Beichuan fault was an active thrust despite very low (within error of zero) geodetic shortening rates (e.g., Shen et al.,

2005). This interpretation was subsequently confirmed by field observations (Densmore et al., 2007), and shortly thereafter the fault ruptured with devastating effects in the 7.9 May 12, 2008 Sichuan earthquake (Burchfiel et al., 2008; Kirby et al., 2008; Zhang et al., 2010). Kirby and Ouimet (2011) have extended and updated the analysis of Kirby et al. (2003) and have shown a powerful linkage between landscape morphology and the deformation pattern associated with the 2008 Sichuan earthquake (Fig. 11a). Similarly, a preliminary analysis of the geomorphic context of the 7.6 October 8, 2005 Muzaffarabad earthquake in Pakistan suggests that the presence of an active thrust capable of generating large earthquakes could have been anticipated if only a quantitative study of the patterns of local relief and channel steepness had been conducted in the region (Fig. 11b). The relative success of these retrodictions in identifying the presence of active structures suggest that we have just begun to tap the potential of the study of the tectonic geomorphology of erosional, high relief landscapes.

4.3. Case study III – transient increase in fault slip in eastern California

It is increasingly apparent that many intracontinental fault systems exhibit strain release patterns that vary with time, ranging from clusters of paleoseismicity (e.g., Rockwell et al., 2000) to long-term variations in fault slip rate (e.g., Friedrich et al., 2003). Such behavior may arise as a consequence of fault growth and interaction (e.g., Roberts and Michetti, 2004), static stress transfer in the upper crust (Stein et al., 1992), changes in surface loading (e.g., Hetzel and Hampel, 2005), switching of fault networks (Bennett et al., 2004; Dolan et al., 2007), or interactions between the earthquake cycle and loading in the deep crust (Osokin et al., 2008). The difficulty of reconstructing changes in displacement through time has limited most studies of the long-term dynamics of interacting fault systems to depositional environments (e.g., Dawers and Underhill, 2000; Gupta et al., 1998; Nicol et al., 2010). In this case study, we show how, in certain settings, the geomorphic response to changes in baselevel driven by fault throw (e.g., Whittaker et al., 2007b) can be used to infer tectonic history.

The high desert ranges of the Inyo and Panamint Mountains, in eastern California, developed as footwall blocks along one of the major fault systems within the Eastern California Shear Zone (Fig. 12a). Right-lateral slip along the Hunter Mountain fault is linked to oblique normal slip along range front faults in both Saline and Panamint Valleys (Fig. 12). Geologic data bracket both the timing of fault initiation between 2.8 and 4.0 Ma (Burchfiel et al., 1987; Lee et al., 2009) and the amount of cumulative displacement between 8 and 10 km (Burchfiel et al., 1987); together these imply that average slip rates along the Hunter Mountain fault have been on the order of 2–4 mm/yr (Lee et al., 2009). However, recent geodetic studies imply present-day strain accumulation of 5–6 mm/yr across the fault system (Gourmelen et al., 2010) suggesting the possibility of an increase in slip rate sometime in the evolution of the fault system (Gourmelen et al., 2011).

Analysis of channel profiles developed in the footwalls of the oblique normal fault segments in both the Inyo and Panamint ranges reveals profiles that appear consistent with a recent increase in throw rate along these fault segments (Kirby et al., 2010). Channels draining across the range front fault in the Inyos exhibit slope-break knickpoints that separate channels into two distinct segments (Fig. 12b); steepness indices (k_{sn}) of the lower segments are approximately twice as steep as upstream segments (Fig. 12c). Channel segments upstream of knickpoints have concavity indices

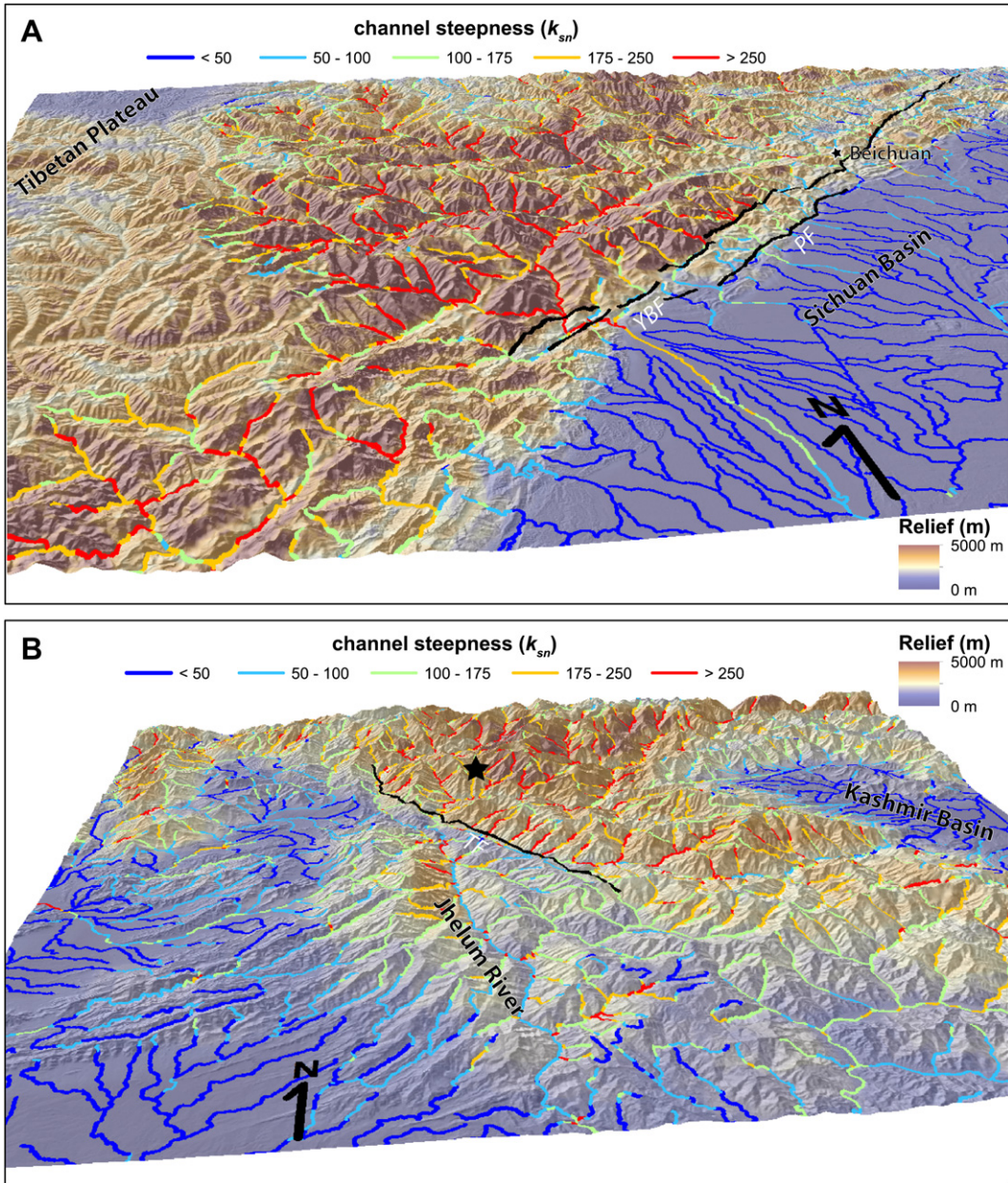


Fig. 11. Topographic context of recent, devastating earthquakes in the Himalaya-Tibet orogen: local relief and channel steepness draped over topography with 1.5 vertical exaggeration. A.) The 2008 Sichuan earthquake in the Longmen Shan, China. Trace of the 2008 Wenchuan surface rupture on Yingxiu-Beichuan (YBF) and Pengguan (PF) faults from Xu et al. (2009) is shown in black. The transition from thrust-dominated oblique slip, to largely dextral strike slip occurs near the former city of Beichuan (star) (Shen et al., 2009). B. The 2005 Muzaffarabad earthquake in Pakistan. Trace of surface rupture along the Tanda fault (TF) along the upper Jhelum River valley and epicenter (star) from Avouac et al. (2006).

(θ) between 0.4 and 0.5, within the range for quasi-equilibrium profiles (Whipple and Tucker, 1999). Channels that do not cross the fault, however, exhibit smooth concave-up profiles with steepness indices that are consistent with upper, relict profiles (light blue symbols, Fig. 12c). Moreover, knickpoints reside in a relatively narrow range of elevations and are independent of lithology, consistent with the expected behavior in response to a sustained forcing.

Reconstruction of channel profiles, coupled with measurements of erosion rate, allows a first order estimate of the timescales associated with this transient incision (Kirby et al., 2010). Projecting the relict profile out to the mountain front yields estimates of the relative change in baselevel of $\sim 500\text{--}900\text{ m}$ (Fig. 13). Erosion rates

determined from ^{10}Be inventories in modern sediment suggest that the “relict” landscape above knickpoints is eroding at relatively low rates ($40\text{--}80\text{ m/Myr}$), whereas erosion rates inferred from concentrations below knickpoints are significantly higher ($>750\text{ m/Myr}$). Making the simple assumption that these rates come close to approximating the present-day rate of relative baselevel fall suggests that the transient incision has been ongoing for 0.5–1 Ma (Fig. 13).

Geologic observations from northern Saline Valley provide preliminary confirmation that this estimate is reasonable. In this region, NW-SE directed extension is distributed among a series of normal faults that cut Plio-Quaternary basalts (Fig. 12a). Using balanced cross-sections, Sternlof (1988) determined that total

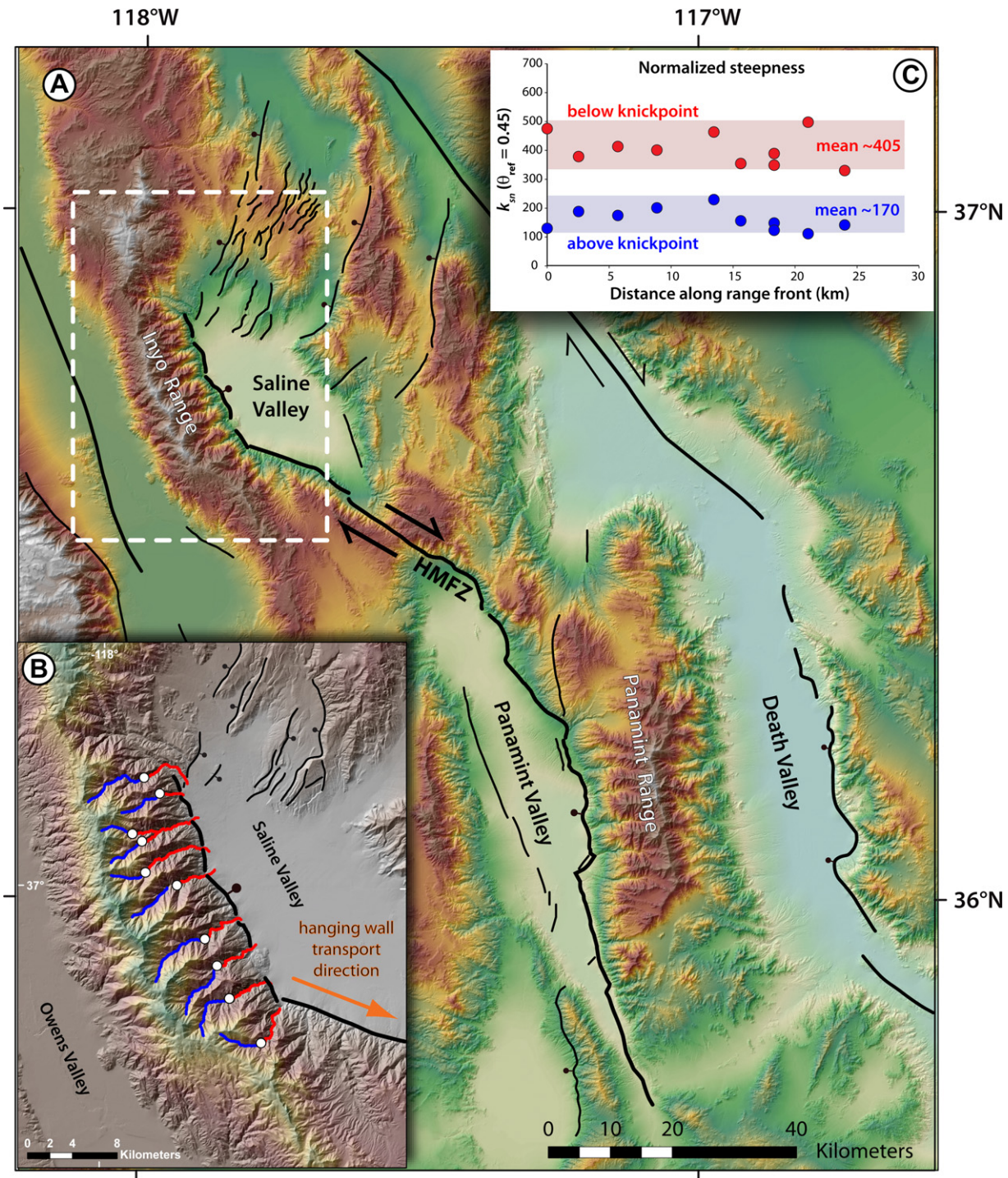


Fig. 12. Example of tectonic geomorphology used to estimate changes in relative baselevel fall across a normal fault system in eastern California (Kirby et al., 2010). A.) Map of active faults in the Panamint Valley – Saline Valley region. B.) Channel profiles in the Inyo Mountains color-coded by steepness index (k_{sn}). Knickpoints are shown as white circles. C.) Channel steepness index for the same drainages (blue – segments upstream of knickpoints; red – segments downstream of knickpoints; light blue – segments that do not cross the range front fault).

extension was 9–10 km in the past 4 Ma, compatible with displacement along the Hunter Mountain fault (Burchfiel et al., 1987). However, the amount of deformation associated with the youngest eruptive units implies that 4.5–5.5 km of this extension accumulated in the past 1.4 Ma (Sternlof, 1988) and appears to require an increase in extension rate. Intriguingly, if all of this slip accrued in the past ~1 Ma, it would yield a slip rate consistent

with the geodetic estimates of 5–6 mm/yr (Gourmelen et al., 2010). Thus, it appears that the present-day high rates of slip along the Hunter Mountain fault system are a relatively young feature of the strain field in eastern California. Although we are still a long way from understanding the dynamics responsible for this behavior, it appears that focused geomorphic analysis has the potential to provide insight into the tempo of active deformation.

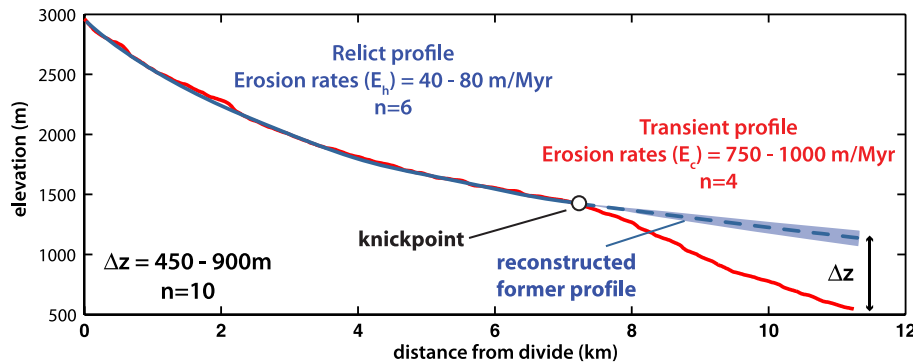


Fig. 13. Example of profile reconstruction in the Inyo range. Channel profile is shown only in range, and is truncated at the trace of the range front fault. The perched landscape above knickpoints is associated with low erosion rates, whereas erosion rates associated with a recent increase in throw rate exceed 750 m/Myr. Using the approach outlined in Fig. 5, Kirby et al. (2010) were able to determine that this increase occurred in the past 0.5–1 Ma.

5. Concluding remarks

In this review, we have tried to show that recent advances in the understanding of how the morphology of actively incising channel profiles can provide powerful reconnaissance insight into the spatial and temporal patterns of deformation. Significant uncertainties remain; the broad outline of the factors that control the quantitative relationship between channel steepness and erosion rate are known, but the exact manner in which substrate erodibility, transport of sediment, channel hydraulic geometry, runoff distribution, and the frequency of debris-flows influence this relationship remain uncertain. As such, direct inversion of channel profiles for uplift histories remains largely a thought exercise, useful to pose hypotheses, but still subject to significant uncertainty. In our opinion, however, there is good reason to believe that thoughtful interpretation of geomorphic patterns can take one a long way toward isolating tectonic signals in the landscape. Moreover, when coupled with focused analysis of erosion rates, such analysis can provide a foundation for distinguishing between spatial and temporal differences in tectonic forcing.

Acknowledgment

We thank the editors of JSG, particularly Tim Horscroft, for both soliciting this review and for patiently seeing it through to completion. Marina Foster Bravo and Mike Zoldak assisted with Figs. 9 and 11, and Scott Miller helped compile data for Fig. 3. Both authors' research has been supported by the Tectonics, Continental Dynamics, and Geomorphology and Land-Use Dynamics programs at NSF. EK acknowledges support from the Alexander von Humboldt Foundation during the writing of this manuscript. Thoughtful reviews by Doug Burbank and Andy Moore helped improve the clarity of the manuscript.

References

- Aalto, R., Dunne, T., Guyot, J.L., 2006. Geomorphic controls on Andean denudation rates. *The Journal of Geology* 114, 85–99.
- Adams, J., 1985. Large-scale tectonic geomorphology of the Southern Alps, New Zealand. In: Morisawa, M., Hack, J.T. (Eds.), *Tectonic Geomorphology*. Allen and Unwin, Boston, pp. 105–128.
- Ahnert, F., 1970. Functional relationships between denudation, relief, and uplift in large mid-latitude drainage basins. *American Journal of Science* 268, 243–263.
- Attal, M., Cowie, P.A., Whittaker, A.C., Hobley, D., Tucker, G.E., Roberts, G.P., 2011. Testing fluvial erosion models using the transient response of bedrock rivers to tectonic forcing in the Apennines, Italy. *Journal of Geophysical Research* 116, F02005.
- Attal, M., Tucker, G.E., Whittaker, A.C., Cowie, P.A., Roberts, G.P., 2008. Modeling fluvial incision and transient landscape evolution: influence of dynamic channel adjustment. *Journal of Geophysical Research-Earth Surface* 113, F03013.
- Avouac, J.-P., Ayoub, F., Leprinse, S., Konca, O., Helmberger, D.V., 2006. The 2005, Mw 7.6 Kashmir earthquake: sub-pixel correlation of ASTER images and seismic waveforms analysis. *Earth and Planetary Science Letters* 249, 514–528.
- Avouac, J.P., 2003. Mountain building, erosion and the seismic cycle in the Nepal Himalaya. *Advances in Geophysics* 46, 1–80.
- Bacon, S.N., McDonald, E.V., Caldwell, T.G., Dalldorf, G.K., 2009. Timing and distribution of alluvial fan sedimentation in response to strengthening of late Holocene ENSO variability in the Sonoran Desert, southwestern Arizona, USA. *Quaternary Research* 73, 425–438.
- Baldwin, J.A., Whipple, K.W., Tucker, G.E., 2003. Implications of the shear stress river incision model for the timescale of postorogenic decay of topography. *Journal of Geophysical Research* 108, 2158.
- Barke, R., Lamb, S., 2006. Late Cenozoic uplift of the eastern Cordillera, Bolivian Andes. *Earth and Planetary Science Letters* 249, 350–367.
- Barnes, J.B., Densmore, A.L., Mukul, M., Sinha, R., Jain, V., Tandon, S.K., 2011. Interplay between faulting and base level in the development of Himalayan frontal fold topography. *Journal of Geophysical Research* 116, F03012.
- Beaumont, C., Fullsack, P., Hamilton, J., 1992. Erosional control of active compressional orogens. In: McClay, K.R. (Ed.), *Thrust Tectonics*. Chapman and Hall, London, pp. 1–18.
- Behr, W.M., Rood, D.H., Fletcher, K.E., Guzman, N., Finkel, R., Hanks, T.C., Hudnut, K.W., Kendrick, K.J., Platt, J.P., Sharp, W.D., Weldon, R.J., Yule, J.D., 2010. Uncertainties in slip-rate estimates for the Mission Creek strand of the southern San Andreas fault at Biskra Palms Oasis, southern California. *Geological Society of America Bulletin* 122, 1360–1377.
- Bennett, R.A., Friedrich, A.M., Furlong, K.P., 2004. Codependent histories of the San Andreas and San Jacinto fault zones from inversion of fault displacement rates. *Geology* 32, 961–964.
- Berlin, M.M., Anderson, R.S., 2007. Modeling of knickpoint retreat on the Roan plateau, western Colorado. *Journal of Geophysical Research-Earth Surface* 112, F03S06.
- Bettinelli, P., Avouac, J.P., Flouzat, M., Jouanne, F., Bollinger, L., Willis, P., Chitrakar, G.R., 2006. Plate motion of India and interseismic strain in the Nepal Himalaya from GPS and DORIS measurements. *Journal of Geodesy* 80, 567–589.
- Bevington, P.R., Robinson, D.K., 1992. *Data Reduction and Error Analysis for the Physical Sciences*, second ed. McGraw-Hill, New York.
- Bierman, P., Steig, E.J., 1996. Estimating rates of denudation using cosmogenic isotope abundances in sediment. *Earth Surface Processes and Landforms* 21, 125–139.
- Bilham, R., Larson, K., Freymueller, J., 1997. GPS measurements of present-day convergence across the Nepal Himalaya. *Nature* 386, 61–63.
- Binnie, S.A., Phillips, W.M., Summerfield, M.A., Fifield, L.K., 2007. Tectonic uplift, threshold hillslopes, and denudation rates in a developing mountain range. *Geology* 35, 743–746.
- Bishop, P., Hoey, T.B., Jansen, J.D., Artza, I.L., 2005. Knickpoint recession rate and catchment area: the case of uplifted rivers in Eastern Scotland. *Earth Surface Processes and Landforms* 30, 767–778.
- Bollinger, L., Avouac, J.P., Beyssac, O., Catlos, E.J., Harrison, T.M., Grove, M., Goffé, B., Sapkota, S., 2004. Thermal structure and exhumation history of the Lesser Himalaya in central Nepal. *Tectonics* 23, TC5015.
- Bollinger, L., Henry, P., Avouac, J.P., 2006. Mountain building in the Nepal Himalaya: thermal and kinematic model. *Earth and Planetary Science Letters* 244, 58–71.
- Bonnet, S., Crave, A., 2003. Landscape response to climate change: insights from experimental modeling and implications for tectonics versus climatic uplift of topography. *Geology* 31, 123–126.
- Bookhagen, B., Burbank, D.W., 2006. Topography, relief, and TRMM-derived rainfall variations along the Himalaya. *Geophysical Research Letters* 33, L08405.

- Bookhagen, B., Burbank, D.W., 2010. Toward a complete Himalayan hydrological budget: spatiotemporal distribution of snowmelt and rainfall and their impact on river discharge. *Journal of Geophysical Research* 115, F03019.
- Bookhagen, B., Strecker, M.R., 2012. Spatiotemporal trends in erosion rates across a pronounced rainfall gradient: examples from the southern Central Andes. *Earth and Planetary Science Letters* 327–328, 97–110.
- Brocklehurst, S.H., Whipple, K.X., 2007. Response of glacial landscapes to spatial variations in rock uplift rate. *Journal of Geophysical Research* 112, F02035.
- Brown, E.T., Stallard, R.F., Larsen, M.C., Raisbeck, G.M., Yiou, F., 1995. Denudation rates determined from the accumulation of in situ-produced ^{10}Be in the Luquillo Experimental Forest, Puerto Rico. *Earth and Planetary Science Letters* 129, 193–202.
- Burbank, D.W., Anderson, R.S., 2001. *Tectonic Geomorphology*. Blackwell, Oxford.
- Burbank, D.W., Leland, J., Fielding, E., Anderson, R.S., Brozovic, N., Reid, M.R., Duncan, C., 1996. Bedrock incision, rock uplift and threshold hillslopes in the northwestern Himalayas. *Nature* 379, 505–510.
- Burchfiel, B.C., Hodges, K.V., Royden, L.H., 1987. Geology of Panamint Valley – Saline Valley pull-apart system, California: palinspastic evidence for low-angle geometry of a Neogene range-bounding fault. *Journal of Geophysical Research* 92, 10,422–10,426.
- Burchfiel, B.C., Royden, L.H., van der Hilst, R.D., Hager, B.H., Chen, Z., King, R.W., Li, C., Li, J., Yao, H., Kirby, E., 2008. A geological and geophysical context for the Wenchuan earthquake of 12 May 2008, Sichuan, People's Republic of China. *Geological Society of America Today* 18, 4–11.
- Cattin, R., Avouac, J.P., 2000. Modeling mountain building and the seismic cycle in the Himalaya of Nepal. *Journal of Geophysical Research* 105, 13389–13407.
- Clark, M.K., Maheo, G., Saleeby, J., Farley, K.A., 2005. The non-equilibrium landscape of the southern Sierra Nevada, California. *GSA Today* 15, 4–10.
- Clarke, B.A., Burbank, D.W., 2010. Bedrock fracturing, threshold hillslopes, and limits to the magnitude of bedrock landslides. *Earth and Planetary Science Letters* 297, 577–586.
- Cook, K.L., Whipple, K., Heimsath, A., Hanks, T.C., 2009. Rapid incision of the Colorado River in Glen Canyon – insights from channel profiles, local incision rates, and modeling of lithologic controls. *Earth Surface Processes and Landforms* 34, 994–1010.
- Cowie, P.A., Attal, M., Tucker, G.E., Whittaker, A.C., Naylor, M., Ganas, A., Roberts, G.P., 2006. Investigating the surface process response to fault interaction and linkage using a numerical modelling approach. *Basin Research* 18, 231–266.
- Craddock, W.H., Burbank, D.W., Bookhagen, B., Gabet, E.J., 2007. Bedrock channel geometry along an orographic rainfall gradient in the upper Marsyandi River valley in central Nepal. *Journal of Geophysical Research-Earth Surface* 112, F03S007.
- Crosby, B.T., Whipple, K.X., 2006. Knickpoint initiation and distribution within fluvial networks: 236 waterfalls in the Waipaoa River, North Island, New Zealand. *Geomorphology* 82, 16–38.
- Crosby, B.T., Whipple, K.X., Gasparini, N.M., Wobus, C.W., 2007. Formation of fluvial hanging valleys: theory and simulation. *Journal of Geophysical Research-Earth Surface* 112, F03S10.
- Cyr, A.J., Granger, D.E., Olivetti, V., Molin, P., 2010. Quantifying rock uplift rates using channel steepness and cosmogenic nuclide-determined erosion rates: examples from northern and southern Italy. *Lithosphere* 2, 188–198.
- Dahlen, F.A., Suppe, J., 1988. Mechanics, growth, and erosion of mountain belts. In: Clark, S.P., Burchfiel, B.C., Suppe, J. (Eds.), *Geologic Society of America Special Paper*, vol. 218. Geologic Society of America, Boulder, CO, pp. 161–178.
- Davis, J.L., Wernicke, B.P., Bisnath, S., Niemi, N.A., Elósegui, P., 2006. Subcontinental-scale crustal velocity changes along the Pacific-North America plate boundary. *Nature* 441, 1131–1134.
- Davis, W.M., 1899. The geographical cycle. *Geographical Journal* 14, 481–504.
- Davis, W.M., 1902. Baselevel, grade and peneplain. *Journal of Geology* 10, 77–111.
- Dawers, N.H., Underhill, J.R., 2000. The role of fault interaction and linkage in controlling synrift stratigraphic sequences: Late Jurassic, Statfjord east area, northern North Sea. *AAPG Bulletin* 84, 45–64.
- Demoulin, A., 1998. Testing the tectonic significance of some parameters of longitudinal river profiles: the case of the Ardenne (Belgium, NW Europe). *Geomorphology* 24, 189–208.
- Densmore, A.L., Anderson, R.S., McAdoo, B.G., Ellis, M.A., 1997. Hillslope evolution by bedrock landslides. *Science* 275, 369–372.
- Densmore, A.L., Dawers, N.H., Gupta, S., Allen, P.A., Gilpin, R., 2003. Landscape evolution at extensional relay zones. *Journal of Geophysical Research* 108, 2273.
- Densmore, A.L., Dawers, N.H., Gupta, S., Guidon, R., Goldin, T., 2004. Footwall topographic development during continental extension. *Journal of Geophysical Research* 109, F03001.
- Densmore, A.L., Ellis, M.A., Li, Y., Zhou, R., Hancock, G.S., Richardson, N., 2007. Active tectonics of the Beichuan and Pengguan faults at the eastern margin of the Tibetan Plateau. *Tectonics* 26, TC4005.
- DiBiase, R.A., Whipple, K.X., 2011. The influence of erosion thresholds and runoff variability on the relationships among topography, climate, and erosion rate. *Journal of Geophysical Research* 116, F04036.
- DiBiase, R.A., Whipple, K.X., Heimsath, A.M., Ouimet, W.B., 2010. Landscape form and millennial erosion rates in the San Gabriel Mountains, CA. *Earth and Planetary Science Letters* 289, 134–144.
- Dietrich, W.E., Bellugi, D.G., Sklar, L.S., Stock, J.D., Heimsath, A.M., Roering, J.J., 2003. Geomorphic transport laws for predicting landscape form and dynamics. In: Wilcock, P.R., Iverson, R.M. (Eds.), *Prediction in Geomorphology*. American Geophysical Union, Washington, DC, pp. 103–132.
- Dixon, T.H., Robaudo, S., Lee, J., Reheis, M.C., 1995. Constraints on present-day Basin and Range deformation from space geodesy. *Tectonics* 14, 755–772.
- Dolan, J.F., Bowman, D.D., Sammis, C.G., 2007. Long-range and long-term fault interactions in Southern California. *Geology* 35, 855–858.
- Dorsey, R.J., Roering, J.J., 2006. Quaternary landscape evolution in the San Jacinto fault zone, Peninsular Ranges of Southern California: transient response to strike-slip fault initiation. *Geomorphology* 73, 16–32.
- Duvall, A., Kirby, E., Burbank, D., 2004. Tectonic and lithologic controls on bedrock channel profiles and processes in coastal California. *Journal of Geophysical Research* 109, F03002.
- England, P., Molnar, P., 1990. Surface uplift, uplift of rocks, and exhumation of rocks. *Geology* 18, 1173–1177.
- Fielding, E.J., Isacks, B.L., Barazangi, M., Duncan, C., 1994. How flat is Tibet? *Geology* 22, 163–167.
- Finnegan, N., Roe, G.H., Montgomery, D.R., Hallet, B., 2005. Controls on the channel width of rivers: implications for modeling fluvial incision of bedrock. *Geology (Boulder)* 33, 229–232.
- Flint, J.J., 1974. Stream gradient as a function of order, magnitude, and discharge. *Water Resources Research* 10, 969–973.
- Foster, D., Brocklehurst, S.H., Gawthorpe, R.L., 2010. Glacial-topographic interactions in the Teton Range, Wyoming. *Journal of Geophysical Research* 115, F01007.
- Friedrich, A.M., Wernicke, B.P., Niemi, N.A., Bennett, R.A., Davis, J.L., 2003. Comparison of geodetic and geologic data from the Wasatch region, Utah, and implications for the spectral character of Earth deformation at periods of 10 to 10 million years. *Journal of Geophysical Research* 108, 2199.
- Gabet, E.J., Pratt-Sitaula, B.A., Burbank, D.W., 2004. Climatic controls on hillslope angle and relief in the Himalayas. *Geology* 32, 629–632.
- Gasparini, N.M., Whipple, K.X., Bras, R.L., 2007. Predictions of steady state and transient landscape morphology using sediment-flux-dependent river incision models. *Journal of Geophysical Research-Earth Surface* 112, F03S09.
- Gilbert, G.K., 1877. *Geology of the Henry Mountains (Utah)*. United States Government Printing Office, Washington, D.C.
- Gold, R.D., Cowgill, E., Arrowsmith, J.R., Gosse, J., Chen, X., Wang, X., Feng, 2009. Riser diachroneity, lateral erosion, and uncertainty in rates of strike-slip faulting: a case study from Tuzidun along the Altyn Tagh Fault, NW China. *Journal of Geophysical Research* 114, B04401.
- Goldrick, G., Bishop, P., 2007. Regional analysis of bedrock stream long profiles: evaluation of Hack's SL form, and formulation and assessment of an alternative (the DS form). *Earth Surface Processes and Landforms* 32, 649–671.
- Goode, J.K., Burbank, D.W., 2009. Numerical study of degradation of fluvial hanging valleys due to climate change. *Journal of Geophysical Research-Earth Surface* 114, F01017.
- Goode, J.K., Burbank, D.W., 2011. Kinematic implications of consequent channels on growing folds. *Journal of Geophysical Research* 116, B04407.
- Gosse, J.C., Phillips, F.M., 2001. Terrestrial in-situ cosmogenic nuclides: theory and application. *Quaternary Science Reviews* 20, 1475–1560.
- Gourmelen, N., Amelung, F., Lanari, R., 2010. Interferometric synthetic aperture radar-GPS integration: interseismic strain accumulation rates across the Hunter Mountain fault in the eastern California shear zone. *Journal of Geophysical Research* 115, B09408.
- Gourmelen, N., Dixon, T.H., Amelung, F., Schmalzle, G., 2011. Acceleration and evolution of faults: an example from the Hunter Mountain-Panamint Valley fault zone, eastern California. *Earth and Planetary Science Letters* 301, 337–344.
- Granger, D.E., Kirchner, J.W., Finkel, R., 1996. Spatially averaged long-term erosion rates measured from in-situ-produced cosmogenic nuclides in alluvial sediment. *Journal of Geology* 104, 249–257.
- Granger, D.E., Riebe, C.S., 2007. Cosmogenic nuclides in weathering and erosion. In: Drever, J.I. (Ed.), *Treatise on Geochemistry*. Elsevier, London.
- Grant-Ludwig, L., Akçiz, S.O., Noriega, G.R., Zielke, O., Arrowsmith, J.R., 2010. Climate-modulated channel incision and rupture history of the San Andreas fault in the Carrizo Plain. *Science* 327, 1117–1119.
- Gupta, S., Cowie, P.A., Dawers, N.H., Underhill, J.R., 1998. A mechanism to explain rift-basin subsidence and stratigraphic patterns through fault-array evolution. *Geology* 26, 595–598.
- Hack, J.T., 1957. Studies of Longitudinal Stream Profiles in Virginia and Maryland, U.S. Geological Survey Professional Paper 294-B, p. 97.
- Hack, J.T., 1973. Stream-profile analysis and stream-gradient index. *Journal of Research of the U.S. Geological Survey* 1, 421–429.
- Hager, B.H., King, R.W., Murray, M.H., 1991. Measurement of crustal deformation using the global positioning system. *Annual Reviews of Earth and Planetary Science* 19, 351–382.
- Hancock, G.S., Anderson, R.S., Whipple, K.X., 1998. Beyond power: bedrock river incision process and form. In: Tinkler, K., Wohl, E.E. (Eds.), *Rivers over Rock: Fluvial Processes in Bedrock Channels*. AGU Press, Washington, D.C., pp. 35–60.
- Harkins, N., Kirby, E., Heimsath, A., Robinson, R., Reiser, U., 2007. Transient fluvial incision in the headwaters of the Yellow River, northeastern Tibet, China. *Journal of Geophysical Research-Earth Surface* 112, F03S04.
- Haviv, I., Enzel, Y., Whipple, K.X., Zilberman, E., Matmon, A., Stone, J., Fifield, K.L., 2010. Evolution of vertical knickpoints (waterfalls) with resistant caprock: insights from numerical modeling. *Journal of Geophysical Research-Earth Surface* 115, F03028.
- Herman, F., Copeland, P., Avouac, J.P., Bollinger, L., Mahéo, G., Le Fort, P., Rai, S., Foster, D., Pécher, A., Stüwe, K., Henry, P., 2010. Exhumation, crustal

- deformation, and thermal structure of the Nepal Himalaya derived from the inversion of thermochronological and thermobarometric data and modeling of the topography. *Journal of Geophysical Research* 115, B06407.
- Hetzel, R., Hampel, A., 2005. Slip rate variations on normal faults during glacial-interglacial changes in surface loads. *Nature* 435, 81–84.
- Hidy, A.J., Gosse, J.C., Pederson, J.L., Mattern, J.P., Finkel, R.C., 2010. A geologically constrained Monte Carlo approach to modeling exposure ages from profiles of cosmogenic nuclides: an example from Lees Ferry, Arizona. *Geochemistry, Geophysics, Geosystems* 11, Q0AA10.
- Hilley, G.E., Arrowsmith, J.R., 2008. Geomorphic response to uplift along the Dragon's Back pressure ridge, Carrizo Plain, California. *Geology (Boulder)* 36, 367–370.
- Hodges, K.V., Wobus, C., Ruhl, K., Schildgen, T., Whipple, K.X., 2004. Quaternary deformation, river steepening, and heavy precipitation at the front of the Higher Himalayan ranges. *Earth and Planetary Science Letters* 7012, 1–11.
- Hoke, G.D., Isacks, B.L., Jordan, T.E., Blanco, N., Tomlinson, A.J., Ramezani, J., 2007. Geomorphic evidence for post-10 Ma uplift of the western flank of the central Andes 18°30'–22°S. *Tectonics* 26, TC5021.
- Howard, A., 1994. A detachment-limited model of drainage basin evolution. *Water Resources Research* 30, 2261–2285.
- Howard, A.D., Dietrich, W.E., Seidl, M.A., 1994. Modeling fluvial erosion on regional to continental scales. *Journal of Geophysical Research-Solid Earth* 99, 13971–13986.
- Howard, A.D., Kerby, G., 1983. Channel changes in badlands. *Geological Society of America Bulletin* 94, 739–752.
- Hurtrez, J.-E., Lucaleau, F., Lave, J., Avouac, J.-P., 1999. Investigation of the relationship between basin morphology, tectonic uplift, and denudation from the study of an active fold belt in the Siwalik Hills, central Nepal. *Journal of Geophysical Research* 104, 12,779–12,796.
- Jackson, M., Bilham, R., 1994. Constraints on Himalayan deformation inferred from vertical velocity fields in Nepal and Tibet. *Journal of Geophysical Research* 99, 13,897–13,912.
- Johnson, C.B., Furlong, K.P., Kirby, E., 2009a. Integrated geomorphic and geodynamic modeling of a potential blind thrust in the San Francisco Bay area, California. *Tectonophysics* 471, 319–328.
- Johnson, J.P., Whipple, K., Sklar, L., Hanks, T.C., 2009b. Transport slopes, sediment cover, and bedrock channel incision in the Henry Mountains, Utah, USA. *Journal of Geophysical Research* 114, F02014.
- Johnson, J.P., Whipple, K.X., 2007. Feedbacks between erosion and sediment transport in experimental bedrock channels: earth Surface Processes and Landforms. *Earth Surface Processes and Landforms* 32, 1048–1062.
- Kirby, E., Johnson, C., Furlong, K., Heimsath, A.M., 2007. Transient channel incision along Bolinas Ridge, California: Evidence for differential rock uplift adjacent to the San Andreas fault. *Journal of Geophysical Research* 112, F03S07.
- Kirby, E., Ouimet, W., 2011. Tectonic geomorphology along the eastern margin of Tibet: insights into the pattern and processes of active deformation adjacent to the Sichuan Basin. In: Gloaguen, R., Ratschbacher, L. (Eds.), *Growth and Collapse of the Tibetan Plateau*. Geological Society, London, pp. 165–188.
- Kirby, E., Regalla, C., Ouimet, W.B., Bierman, P.R., 2010. Reconstructing Temporal Variation in Fault Slip from Footwall Topography: An Example from Saline Valley, California, 2010 Fall Meeting, American Geophysical Union, San Francisco, CA.
- Kirby, E., Whipple, K., 2001. Quantifying differential rock-uplift rates via stream profile analysis. *Geology* 29, 415–418.
- Kirby, E., Whipple, K., Harkins, N., 2008. Topography reveals seismic hazard. *Nature Geoscience* 1, 485–487.
- Kirby, E., Whipple, K., Tang, W., Chen, Z., 2003. Distribution of active rock uplift along the eastern margin of the Tibetan Plateau: inferences from bedrock channel longitudinal profiles. *Journal of Geophysical Research* 108, 2217.
- Klinger, Y., Etchebehere, M., Tapponnier, P., Narteau, C., 2011. Characteristic slip for five great earthquakes along the Fuyun fault in China. *Nature Geoscience* 4, 389–392.
- Koons, P.O., 1989. The topographic evolution of collisional mountain belts: a numerical look at the Southern Alps, New Zealand. *American Journal of Science* 289, 1041–1069.
- Koons, P.O., 1990. Two-sided orogen: collision and erosion from the sandbox to the Southern Alps, New Zealand. *Geology* 18, 679–682.
- Koons, P.O., Kirby, E., 2007. Topography, denudation, and deformation. In: Handy, M.R., Hirth, G., Hovius, N. (Eds.), *Tectonic Faults: Agents of Change on a Dynamic Earth*. MIT Press, Cambridge, MA, pp. 205–230.
- Korup, O., 2006. Rock-slope failure and the river long profile. *Geology* 34, 45–48.
- Korup, O., Montgomery, D.R., Hewitt, K., 2010. Glacier and landslide feedbacks to topographic relief in the Himalayan syntaxes. *Proceedings of the National Academy of Sciences* 107, 5317–5322.
- Lague, D., 2010. Reduction of long-term bedrock incision efficiency by short-term alluvial cover intermittency. *Journal of Geophysical Research-Earth Surface* 115.
- Lague, D., Davy, P., 2003. Constraints on the long-term colluvial erosion law by analyzing slope-area relationships at various tectonic uplift rates in the Siwalik Hills (Nepal). *Journal of Geophysical Research* 108, 2129.
- Lague, D., Hovius, N., Davy, P., 2005. Discharge, discharge variability, and the bedrock channel profile. *Journal of Geophysical Research* 110. <http://dx.doi.org/10.1029/2004JF000259>.
- Larson, K.M., Burgmann, R., Bilham, R., Freymueller, J.T., 1999. Kinematics of the India-Eurasia collision zone from GPS measurements. *Journal of Geophysical Research* 104, 1077–1093.
- Lavé, J., Avouac, J.P., 2000. Active folding of fluvial terraces across the Siwalik Hills, Himalayas of central Nepal. *Journal of Geophysical Research* 105, 5735–5770.
- Lavé, J., Avouac, J.P., 2001. Fluvial incision and tectonic uplift across the Himalayas of central Nepal. *Journal of Geophysical Research* 106, 26,561–526,591.
- Lee, J., Stockli, D.F., Owen, L.A., Finkel, R.C., Kislistyn, R., 2009. Exhumation of the Inyo Mountains, California: implications for the timing of extension along the western boundary of the Basin and Range province and distribution of dextral fault slip rates across the eastern California shear zone. *Tectonics* 28, TC1001.
- Lensen, G.J., 1964. The general case of progressive fault displacement of flights of degradational terraces. *New Zealand Journal of Geology and Geophysics* 7, 864–870.
- Mackin, J.H., 1948. Concept of the graded river. *Geological Society of America Bulletin* 101, 1373–1388.
- Matmon, A., Bierman, P.R., Larsen, J., Southworth, S., Pavich, M.J., Caffee, M.W., 2003. Temporally and spatially uniform rates of erosion in the southern Appalachian Great Smoky Mountains. *Geology* 31, 155–158.
- Meade, B.J., 2010. The signature of an unbalanced earthquake cycle in Himalayan topography? *Geology* 38, 987–990.
- Meade, B.J., Hager, B.H., 2005. Block models of crustal motion in southern California constrained by GPS measurements. *Journal of Geophysical Research* 110, B03403.
- Medwedeff, D.A., Suppe, J., 1997. Multibend fault-bend folding. *Journal of Structural Geology* 19, 279–292.
- Merritts, D., Vincent, K.R., 1989. Geomorphic response of coastal streams to low, intermediate, and high rates of uplift, Mendocino junction region, northern California. *Geological Society of America Bulletin* 101, 1373–1388.
- Miller, S.R., Baldwin, S.L., Fitzgerald, P.G., 2012. Transient fluvial incision and active surface uplift in the Woodlark Rift of eastern Papua New Guinea. *Lithosphere* 4, 131–149.
- Miller, S.R., Sak, P.B., Kirby, E., Bierman, P.R., 2011. Bumps in the long road to flat, American Geophysical Union, Fall Meeting 2011, San Francisco, CA.
- Miller, S.R., Slingerland, R.L., Kirby, E., 2007. Characteristics of steady state fluvial topography above fault bend folds. *Journal of Geophysical Research* 112, F04004.
- Mishra, P., Mukhopadhyay, D.K., 2002. Balanced structural models of Mohand and Santaugurh ramp anticlines, Himalayan foreland fold-thrust belt, Dehra Dun re-entrant, Uttarakhand. *Journal Geological Society of India* 60, 649–661.
- Moglen, G.E., Bras, R.L., 1995. The effect of spatial heterogeneities on geomorphic expression in a model of basin evolution. *Water Resources Research* 31, 2613–2623.
- Molnar, P., 1987. Inversion of profiles of uplift rates for the geometry of dip-slip faults at depth, with examples from the Alps and Himalaya. *Annales Geophysicae* 5B, 663–670.
- Montgomery, D.R., Foufoula-Georgiou, E., 1993. Channel network representation using digital elevation models. *Water Resources Research* 29, 1178–1191.
- Morell, K.D., Kirby, E., Fisher, D.M., van Soest, M., 2012. Geomorphic and exhumational response of the Central American Volcanic Arc to Cocos Ridge subduction. *Journal of Geophysical Research* 117, B04409.
- Ni, J., Barazangi, M., 1984. Seismotectonics of the Himalayan collision zone: geometry of the underthrusting Indian plate beneath the Himalaya. *Journal of Geophysical Research* 89, 1147–1163.
- Nicol, A., Walsh, J.J., Villamor, P., Seebeck, H., Berryman, K.R., 2010. Normal fault interactions, paleoearthquakes, and growth in an active rift. *Journal of Structural Geology* 32, 1101–1113.
- Niemann, J.D., Gasparini, N.M., Tucker, G.E., Bras, R.L., 2001. A quantitative evaluation of Playfair's law and its use in testing long-term stream erosion models. *Earth Surface Processes and Landforms* 26, 1317–1332.
- Niemi, N.A., Oskin, M., Burbank, D.W., Heimsath, A.M., Gabet, E.J., 2005. Effects of bedrock landslides on cosmogenically determined erosion rates. *Earth and Planetary Science Letters* 237, 480–498.
- Olivetti, V., Cyr, A.J., Molin, P., Faccenna, C., Granger, D.E., 2012. Uplift history of the Sila Massif, southern Italy, deciphered from cosmogenic 10Be erosion rates and river longitudinal profile analysis. *Tectonics* 31, TC3007.
- Oskin, M., Burbank, D.W., 2005. Alpine landscape evolution dominated by cirque retreat. *Geology* 33, 933–936.
- Oskin, M., Perg, L., Shelef, E., Strane, M., Gurney, E., Singer, G., Zhang, X., 2008. Elevated shear zone loading rate during an earthquake cluster in eastern California. *Geology* 36, 507–510.
- Ouimet, W.B., Whipple, K.X., Granger, D.E., 2009. Beyond threshold hillslopes: channel adjustment to base-level fall in tectonically active mountain ranges. *Geology* 37, 579–582.
- Ouimet, W.B., Whipple, K.X., Royden, L.H., Sun, Z., Chen, Z., 2007. The influence of large landslides on river incision in a transient landscape: eastern margin of the Tibetan Plateau (Sichuan, China). *Geological Society of America Bulletin* 119, 1462–1476.
- Pan, B., Burbank, D.W., Wang, Y., Wu, G., Li, J., Guan, Q., 2003. A 900 k.y. Record of strath terrace formation during glacial-interglacial transitions in northwest China. *Geology* 31, 957–960.
- Pandey, M.R., Tandukar, R.P., Avouac, J.P., Lave, J., Massot, J.P., 1995. Interseismic strain accumulation on the Himalayan crustal ramp (Nepal). *Geophysical Research Letters* 22, 751–754.
- Peltzer, G., Tapponnier, P., 1988. Formation and evolution of strike-slip faults, rifts and basins during the India - Asia collision: an experimental approach. *Journal of Geophysical Research* 93, 15095–15117.
- Penck, W., 1953. *Morphological Analysis of Landforms*. St. Martin's Press, New York.

- Portenga, E.W., Bierman, P.R., Reusser, L., 2011. Understanding Earth's eroding surface with ^{10}Be . *GSA Today* 21, 4–10.
- Powers, P.M., Lillie, R.J., Yeats, R.S., 1998. Structure and shortening of the Kangra and Dehra Dun reentrants, Sub-Himalaya, India. *Geological Society of America Bulletin* 110, 1010–1027.
- Raiberman, V., Mukerjea, A., Saproo, M.K., Kunte, S.V., Ram, J., 1990. Geological Map of Himalayan Foothills between Yamuna and Sarda Rivers. Institute of Petroleum Exploration, Dehra Dun, India.
- Reinhardt, L.J., Bishop, P., Hoey, T.B., Dempster, T.J., Sanderson, D.C.W., 2007. Quantification of the transient response to base-level fall in a small mountain catchment: Sierra Nevada, southern Spain. *Journal of Geophysical Research-Earth Surface* 112, F03S05.
- Reusser, L.J., Bierman, P.R., Pavich, M.J., Zen, E.A., Larsen, J., Finkel, R., 2004. Rapid late Pleistocene incision of Atlantic passive-margin river gorges. *Science* 305, 499–502.
- Robert, X., van der Beek, P., Braun, J., Perry, C., Dubille, M., Mugnier, J.-L., 2009. Assessing Quaternary reactivation of the Main Central thrust zone (central Nepal Himalaya): new thermochronologic data and numerical modeling. *Geology* 37, 731–734.
- Roberts, G.P., Michetti, A.M., 2004. Spatial and temporal variations in growth rates along active normal fault systems: an example from the Lazio-Abruzzo Apennines, central Italy. *Journal of Structural Geology* 26, 339–376.
- Rockwell, T.K., Keller, E.A., Clark, M.N., Johnson, D.L., 1984. Chronology and rates of faulting of Ventura River terraces, California. *Geological Society of America Bulletin* 95, 1466–1474.
- Rockwell, T.K., Lindvall, S., Herzberg, M., Murbach, D., Dawson, T., Berger, G., 2000. Paleoseismology of the Johnson Valley, Kickapoo, and Homestead Valley faults: clustering of earthquakes in the Eastern California Shear Zone. *Bulletin of the Seismological Society of America* 90, 1200–1236.
- Roe, G.H., Montgomery, D.R., Hallet, B., 2002. Effects of orographic precipitation variations on the concavity of steady-state river profiles. *Geology (Boulder)* 30, 143–146.
- Rosenbloom, N.A., Anderson, R.S., 1994. Hillslope and channel evolution in a marine terraced landscape, Santa Cruz, California. *Journal of Geophysical Research* 99, 14,013–14,029.
- Rossi, M.W., Whipple, K.X., DiBiase, R.A., Heimsath, A.M., 2011. Climatic Controls on Steady State Erosion using the Relationship between Channel Steepness and Cosmogenic ^{10}Be -derived Catchment Averaged Erosion Rates, 2011 Fall Meeting, AGU, American Geophysical Union, San Francisco, CA.
- Royden, L.H., Clark, M.K., Whipple, K.X., 2000. Evolution of River Elevation Profiles by Bedrock Incision: Analytical Solutions for Transient River Profiles Related to Changing Uplift and Precipitation Rates. *EOS, Transactions American Geophysical Union* 81, Fall Meeting Supplement, Abstract T62F-09.
- Safran, E.B., Bierman, P.R., Aalto, R., Dunne, T., Whipple, K., Caffee, M., 2005. Erosion rates driven by channel network incision in the Bolivian Andes. *Earth Surface Processes and Landforms* 30, 1007–1024.
- Schildgen, T.F., Cosentino, D., Bookhagen, B., Niedermann, S., Yildirm, C., Echtler, H.P., Strecker, M.R., 2012. Multi-phased uplift of the southern margin of the Central Anatolian plateau, Turkey: a record of tectonic and upper mantle processes. *Earth and Planetary Science Letters* 317–318, 85–95.
- Schlunegger, F., Norton, K.P., Zeilinger, G., 2011. Climatic forcing on channel profiles in the Eastern Cordillera of the Coroico region, Bolivia. *Journal of Geology* 119, 97–107.
- Schmidt, K.M., Montgomery, D.R., 1995. Limits to relief. *Science* 270, 617–619.
- Schoenbohm, L.M., Whipple, K.X., Burchfiel, B.C., Chen, L., 2004. Geomorphic constraints on surface uplift, exhumation, and plateau growth in the Red River region, Yunnan Province, China. *Geological Society of America Bulletin* 116, 895–909.
- Seeber, L., Armbruster, J., 1981. Great Detachment Earthquakes along the Himalayan Arc and Long-term Forecasting, Earthquake Prediction: An International Review. American Geophysical Union, Washington D.C., pp. 259–279.
- Seeber, L., Gornitz, V., 1983. River profiles along the Himalayan Arc as indicators of active tectonics. *Tectonophysics* 92, 335–367.
- Seidl, M.A., Dietrich, W.E., 1992. The problem of channel erosion into bedrock. *Catena Supplement* 23, 101–124.
- Shafizad, F., Gloaguen, R., 2011. TecDEM: a MATLAB based toolbox for tectonic geomorphology, Part 1: drainage network preprocessing and stream profile analysis. *Computers and Geosciences* 37, 250–260.
- Shen, Z.-K., Lü, J., Wang, M., Bürgmann, R., 2005. Contemporary crustal deformation around the southeast borderland of the Tibetan Plateau. *Journal of Geophysical Research* 110, B11409.
- Shen, Z.-K., Sun, J., Zhang, P., Wan, Y., Wang, M., Bürgmann, R., Zeng, Y., Gan, W., Liao, H., Wang, Q., 2009. Slip maxima at fault junctions and rupturing of barriers during the 2008 Wenchuan earthquake. *Nature Geoscience* 2, 718–724.
- Sklar, L., Dietrich, W.E., 1998. River longitudinal profiles and bedrock incision models: stream power and the influence of sediment supply. In: Tinkler, K.J., Wohl, E.E. (Eds.), *Rivers over Rock: Fluvial Processes in Bedrock Channels*. AGU Press, Washington, D.C., pp. 237–260.
- Sklar, L., Dietrich, W.E., 2004. A mechanistic model for river incision into bedrock by saltating bed load. *Water Resources Research* 40, W06301.
- Sklar, L.S., Dietrich, W.E., 2006. The role of sediment in controlling steady-state bedrock channel slope: implications of the saltation-abrasion incision model. *Geomorphology* 82, 58–83.
- Snow, R.S., Slingerland, R.L., 1987. Mathematical modeling of graded river profiles. *Journal of Geology* 95, 15–33.
- Snyder, N., Whipple, K., Tucker, G., Merritts, D., 2000. Landscape response to tectonic forcing: digital elevation model analysis of stream profiles in the Mendocino triple junction region, northern California. *Geological Society of America, Bulletin* 112, 1250–1263.
- Snyder, N.P., Whipple, K.X., Tucker, G.E., Merritts, D.J., 2003a. Channel response to tectonic forcing: field analysis of stream morphology and hydrology in the Mendocino triple junction region, northern California. *Geomorphology* 53, 97–127.
- Snyder, N.P., Whipple, K.X., Tucker, G.E., Merritts, D.J., 2003b. Importance of a stochastic distribution of floods and erosion thresholds in the bedrock river incision problem. *Journal of Geophysical Research* 108, 2117.
- Snyder, N.P., Whipple, K.X., Tucker, G.E., Merritts, D.M., 2002. Interactions between onshore bedrock-channel incision and nearshore wave-base erosion forced by eustacy and tectonics. *Basin Research* 14, 105–127.
- Sorby, A.P., England, P.C., 2004. Critical Assessment of Quantitative Geomorphology in the Footwall of Active Normal Faults, Basin and Range Province, Western USA. *EOS Transactions American Geophysical Union* 85, Fall Meeting Supplement, Abstract T42B-02.
- Spotila, J.A., House, M.A., Blythe, A.E., Niemi, N.A., Bank, G.C., 2002. Controls on the erosion and geomorphic evolution of the San Bernardino and San Gabriel Mountains, southern California. *Geological Society American Special Paper* 365, 205–230.
- Stark, C.P., 2006. A self-regulating model of bedrock river channel geometry. *Geophysical Research Letters* 33, L04402.
- Stein, R.S., King, G.C.P., Lin, J., 1992. Change in failure stress on the southern San Andreas fault system caused by the 1992 magnitude = 7.4 Landers earthquake. *Science* 258, 1328–1332.
- Sternlieb, I.R., 1988. Structural Style and Kinematic History of the Active Panamint-Saline Extensional System, Inyo County, California. MIT, Cambridge, MA, p. 40.
- Stock, J., Dietrich, W.E., 2003. Valley incision by debris flows: evidence of a topographic signature. *Water Resources Research* 39, 1089.
- Stolar, D.B., Willett, S.D., Roe, G.H., 2006. Climatic and tectonic forcing of a critical orogen. In: Willett, S.D., Hovius, N., Brandon, M.T., Fisher, D.M. (Eds.), *Tectonics, Climate, and Landscape Evolution*. Geological Society of America Special Paper, vol. 398, pp. 241–250.
- Strahler, A.N., 1950. Equilibrium theory of erosional slopes approached by frequency distribution analysis: Part 1. *American Journal of Science* 248, 673–696.
- Tapponnier, P., Molnar, P., 1977. Active faulting and tectonics in China. *Journal of Geophysical Research* 82, 2905–2930.
- Tressler, C., 2011. From Hillslopes to Canyons, Studies of Erosion at Differing Time and Spatial Scales within the Colorado River Drainage, *Geology*. Utah State University, p. 99.
- Tucker, G., 2004. Drainage basin sensitivity to tectonic and climatic forcing: implications of a stochastic model for the role of entrainment and erosion thresholds. *Earth Surface Processes and Landforms* 29, 185–205.
- Tucker, G.E., Whipple, K.X., 2002. Topographic outcomes predicted by stream erosion models: sensitivity analysis and intermodel comparison. *Journal of Geophysical Research* 107, 2179.
- Turowski, J.M., Lague, D., Hovius, N., 2007. Cover effect in bedrock abrasion: a new derivation and its implications for the modeling of bedrock channel morphology. *Journal of Geophysical Research-Earth Surface* 112, F04006.
- Van der Woerd, J., Tapponnier, P., Ryerson, F.J., Meriaux, A.-S., Meyer, B., Gaudemer, Y., Finkel, R.C., Caffee, M.W., Zhao, G., Xu, Z., 2002. Uniform post-glacial slip-rate along the central 600 km of the Kunlun Fault (Tibet), from ^{20}Al , ^{10}Be , and ^{14}C dating of riser offsets, and climatic origin of the regional morphology. *Geophysical Journal International* 148, 356–388.
- Wager, L.R., 1933. The rise of the Himalaya. *Nature* 132, 28.
- Wager, L.R., 1937. The Arun river drainage pattern and the rise of the Himalaya. *Geographical Journal* 89, 239–250.
- Walcek, A.A., Hoke, G.D., 2012. Surface uplift and erosion of the southernmost Argentine Precordillera. *Geomorphology* 153–154, 156–168.
- Wallace, R.E., 1977. Profiles and ages of young fault scarps, north-central Nevada. *Geological Society of America Bulletin* 88, 1267–1281.
- Wesnousky, S.G., Kumar, S., Mohindra, R., Thakur, V.C., 1999. Uplift and convergence along the Himalayan frontal thrust of India. *Tectonics* 18, 967–976.
- Whipple, K., 2001. Fluvial landscape response time: how plausible is steady state denudation? *American Journal of Science* 301, 313–325.
- Whipple, K., 2004. Bedrock rivers and the geomorphology of active orogens. *Annual Review of Earth and Planetary Sciences* 32, 151–185.
- Whipple, K., 2009. The influence of climate on the tectonic evolution of mountain belts. *Nature Geoscience* 2, 97–104.
- Whipple, K., Tucker, G., 2002. Implications of sediment-flux dependent river incision models for landscape evolution. *Journal of Geophysical Research* 107.
- Whipple, K.X., DiBiase, R., Crosby, B., 2011. Bedrock rivers. In: Owen, L. (Ed.), *Treatise in Fluvial Geomorphology*.
- Whipple, K.X., Hancock, G.S., Anderson, R.S., 2000. River incision into bedrock: mechanics and relative efficacy of plucking, abrasion, and cavitation. *Geological Society of America Bulletin* 112, 490–503.
- Whipple, K.X., Kirby, E., Brocklehurst, S.H., 1999. Geomorphic limits to climate-induced increases in topographic relief. *Nature* 401, 39–43.
- Whipple, K.X., Tucker, G.E., 1999. Dynamics of the stream-power river incision model: implications for height limits of mountain ranges, landscape response timescales, and research needs. *Journal of Geophysical Research* 104, 17661–17674.

- Whittaker, A.C., Attal, M., Allen, P.A., 2010. Characterising the origin, nature and fate of sediment exported from catchments perturbed by active tectonics. *Basin Research* 22, 809–828.
- Whittaker, A.C., Attal, M., Cowie, P.A., Tucker, G.E., Roberts, G.P., 2008. Decoding temporal and spatial patterns of fault uplift using transient river long profiles. *Geomorphology* 100, 506–526.
- Whittaker, A.C., Boulton, S.J., 2012. Tectonic and climatic controls on knickpoint retreat rates and landscape response times. *Journal of Geophysical Research* 117, F02024.
- Whittaker, A.C., Cowie, P.A., Attal, M., Tucker, G.E., Roberts, G.P., 2007a. Bedrock channel adjustment to tectonic forcing: implications for predicting river incision rates. *Geology* 35, 103–106.
- Whittaker, A.C., Cowie, P.A., Attal, M., Tucker, G.E., Roberts, G.P., 2007b. Contrasting transient and steady-state rivers crossing active normal faults: new field observations from the Central Apennines, Italy. *Basin Research* 19, 529–556.
- Willett, S.D., 1999. Orogeny and orography: the effects of erosion on the structure of mountain belts. *Journal of Geophysical Research* 104, 28,957–928,981.
- Willett, S.D., Brandon, M.T., 2002. On steady states in mountain belts. *Geology* 30, 175–178.
- Wobus, C., Heimsath, A., Whipple, K., Hodges, K., 2005. Active out-of-sequence thrust faulting in the central Nepalese Himalaya. *Nature* 434, 1008–1011.
- Wobus, C., Whipple, K.X., Kirby, E., Snyder, N., Johnson, J., Spyropoulos, K., Crosby, B., Sheehan, D., 2006a. Tectonics from topography: procedures, promise, and pitfalls. In: Willett, S.D., Hovius, N., Brandon, M.T., Fisher, D.M. (Eds.), *Tectonics, Climate, and Landscape Evolution*. Geological Society of America Special Paper, vol. 398, pp. 55–74.
- Wobus, C.W., Crosby, B.T., Whipple, K.X., 2006b. Hanging valleys in fluvial systems: controls on occurrence and implications for landscape evolution. *Journal of Geophysical Research-Earth Surface* 111, F02017.
- Wobus, C.W., Hodges, K.V., Whipple, K.X., 2003. Has focused denudation sustained active thrusting at the Himalayan topographic front? *Geology* 10, 861–864.
- Wobus, C.W., Tucker, G.E., Anderson, R.S., 2006c. Self-formed bedrock channels. *Geophysical Research Letters* 33, L18408.
- Wobus, C.W., Whipple, K.X., Hodges, K.V., 2006d. Neotectonics of the central Nepalese Himalaya: constraints from geomorphology, detrital 40Ar/39Ar thermochronology, and thermal modeling. *Tectonics* 25, TC4011.
- Xu, X., Wen, X., Yu, G., Chen, G., Klinger, Y., Hubbard, J., Shaw, J., 2009. Coseismic reverse- and oblique-slip surface faulting generated by the 2008 Mw 7.9 Wenchuan earthquake, China. *Geology* 37, 515–518.
- Zaprowski, B.J., Pazzaglia, F.J., Evenson, E.B., 2005. Climatic influences on profile concavity and river incision. *Journal of Geophysical Research-Earth Surface* 110.
- Zhang, P., Wen, X., Shen, Z.-K., Chen, J., 2010. Oblique, high-angle listric-reverse faulting and associated development of strain: The Wenchuan earthquake of May 12, 2008, Sichuan, China. *Annual Reviews of Earth and Planetary Science* 28, 351–380.
- Zhang, P.-Z., Shen, Z.-k., Wang, M., Gan, W., Burgmann, R., Molnar, P., Wang, Q., Niu, Z., Sun, J., Wu, J., Hanrong, S., Xinzhaoy, Y., 2004. Continuous deformation of the Tibetan Plateau from global positioning system data. *Geology* 32, 809–812.
- Zielke, O., Arrowsmith, J.R., Grant-Ludwig, L., Akçiz, S.O., 2010. Slip in the 1857 and earlier large earthquakes along the Carrizo Plain, San Andreas fault. *Science* 327, 1119–1122.